1. Report No. CA18-2911	2. Government Accession No.	3. Recipient's Catalog No.	
4. Title and Subtitle Using Cooperative Adaptive Cruise Control (CACC) to Form High-Performance Vehicle Streams—Final Report		5. Report Date March 2018	
		6. Performing Organization Code	
7. Author(s) Hao Liu, Lin Xiao, Xingan (David) Kan, Steven E. Shladover, Xiao-Yun Lu, Meng Wang, Wouter Schakel, Bart van Arem		8. Performing Organization Report No.	
9. Performing Organization Name and Address California PATH Program, Institute of Transportation Studies, University of California, Berkeley, Richmond Field Station, 1357 S. 46th Street, Richmond, CA 94804 Faculty of Civil Engineering and Geosciences, Department of Transport & Planning, Delft University of Technology, Stevinweg 1, 2628 CN Delft, The Netherlands		10. Work Unit No. (TRAIS)	
		11. Contract or Grant No. DTFH61-13-H-00013	
12. Sponsoring Agency Name and Address Federal Highway Administration – Exploratory Advanced Research Program Turner-Fairbank Highway Research Center 6300 Georgetown Pike McLean, VA 22101		13. Type of Report and Period Covered Final Report	
		14. Sponsoring Agency Code	
15. Supplementary Notes			

16. Abstract

Freeway capacity and throughput can be significantly improved via CACC vehicle string operations. This research aims to provide authoritative predictions regarding impacts of CACC on traffic flow and quantitative estimations of the influences of CACC operation strategies that might create the capacity and throughput improvement in the freeway traffic stream. To this end, the PATH and Delft team have independently developed micro simulation platforms that represent the behaviors of CACC vehicles and their interactions with human drivers. The models have been calibrated using archived data from a complicated 13-mile long section of the northbound SR-99 freeway near Sacramento, California for an 8-hour period in which the traffic fluctuated between free-flow and congested conditions. Calibration results show extremely good agreement between field data and model predictions. The models have been cross-validated and produced similar macroscopic traffic performance. With the simulation platforms, we have explored the effects of CACC under various market penetrations and the impacts of a CACC managed lane (ML) strategy, a vehicle awareness device (VAD) strategy and discretionary lane change (DLC) restrictions on the traffic flow dynamics of a simple four-lane freeway section and the 13-mile freeway corridor. Results from both models reveal that the freeway capacity increases quadratically as the CACC market penetration increases, with a maximum value of 3080 veh/hr/lane at 100% market penetration. The disturbance from the on-ramp traffic causes the merge bottleneck and can reduce the freeway capacity by up to 13% but the bottleneck capacity still increases on a quadratic trend as CACC market penetration becomes larger. The results also indicate that the ML and VAD strategy can substantially increase the pipeline capacity of the freeway when the CACC market penetration is 60% or less. On the other hand, the DLC restriction strategy is most helpful when the penetration is 80% or higher. The ML and VAD strategy can lead to significant improvement of the traffic operation at freeway on-ramp bottlenecks under various CACC market penetration cases. Those strategies are also capable of enhancing the overall operation of the freeway corridor, even for CACC market penetrations as low as 20%.

17. Key Words Cooperative Adaptive Cruise Control (CACC), microscopic traffic modeling, model calibration and validation, CACC vehicle string operation strategies, traffic impact analyses		18. Distribution Statement No restrictions. This document is available to the public through the National Technical Information Service Alexandria, Virginia 22312	
19. Security Classif.(of this report) Unclassified	20. Security Classif.(of this page) Unclassified	21. No. of Pages 56	22. Price

Form DOT F 1700.7 (8-72)   **Reproduction of completed page authorized**

DISCLAIMER STATEMENT

Using Cooperative Adaptive Cruise Control (CACC) to Form High-Performance Vehicle Streams

FINAL REPORT

March 2018

Hao Liu

Lin Xiao

Xingan (David) Kan

Steven E. Shladover

Xiao-Yun Lu

Meng Wang

Wouter Schakel

Bart van Arem

California PATH Program

Institute of Transportation Studies

University of California, Berkeley

SI* (MODERN METRIC) CONVERSION FACTORS

APPROXIMATE CONVERSIONS TO SI UNITS

Symbol	When You Know	Multiply By	To Find	Symbol
LENGTH				
in	inches	25.4	millimeters	mm
ft	feet	0.305	meters	m
yd	yards	0.914	meters	m
mi	miles	1.61	kilometers	km
AREA				
in^2	square inches	645.2	square millimeters	mm^2
ft^2	square feet	0.093	square meters	m^2
yd^2	square yard	0.836	square meters	m^2
ac	acres	0.405	hectares	ha
mi^2	square miles	2.59	square kilometers	km^2
VOLUME				
fl oz	fluid ounces	29.57	milliliters	mL
gal	gallons	3.785	liters	L
ft^3	cubic feet	0.028	cubic meters	m^3
yd^3	cubic yards	0.765	cubic meters	m^3
NOTE: volumes greater than 1000 L shall be shown in m^3				
MASS				
oz	ounces	28.35	grams	g
lb	pounds	0.454	kilograms	kg
T	short tons (2000 lb)	0.907	megagrams (or "metric ton")	Mg (or "t")
TEMPERATURE (exact degrees)				
°F	Fahrenheit	5 (F-32)/9 or (F-32)/1.8	Celsius	°C
ILLUMINATION				
fc	foot-candles	10.76	lux	lx
fl	foot-Lamberts	3.426	candela/m^2	cd/m^2
FORCE and PRESSURE or STRESS				
lbf	poundforce	4.45	newtons	N
lbf/in^2	poundforce per square inch	6.89	kilopascals	kPa

APPROXIMATE CONVERSIONS FROM SI UNITS

Symbol	When You Know	Multiply By	To Find	Symbol
LENGTH				
mm	millimeters	0.039	inches	in
m	meters	3.28	feet	ft
m	meters	1.09	yards	yd
km	kilometers	0.621	miles	mi
AREA				
mm^2	square millimeters	0.0016	square inches	in^2
m^2	square meters	10.764	square feet	ft^2
m^2	square meters	1.195	square yards	yd^2
ha	hectares	2.47	acres	ac
km^2	square kilometers	0.386	square miles	mi^2
VOLUME				
mL	milliliters	0.034	fluid ounces	fl oz
L	liters	0.264	gallons	gal
m^3	cubic meters	35.314	cubic feet	ft^3
m^3	cubic meters	1.307	cubic yards	yd^3
MASS				
g	grams	0.035	ounces	oz
kg	kilograms	2.202	pounds	lb
Mg (or "t")	megagrams (or "metric ton")	1.103	short tons (2000 lb)	T
TEMPERATURE (exact degrees)				
°C	Celsius	1.8C+32	Fahrenheit	°F
ILLUMINATION				
lx	lux	0.0929	foot-candles	fc
cd/m^2	candela/m^2	0.2919	foot-Lamberts	fl
FORCE and PRESSURE or STRESS				
N	newtons	0.225	poundforce	lbf
kPa	kilopascals	0.145	poundforce per square inch	lbf/in^2

*SI is the symbol for the International System of Units. Appropriate rounding should be made to comply with Section 4 of ASTM E380.
(Revised March 2003)

TABLE OF CONTENTS

LIST OF FIGURES

LIST OF TABLES

LIST OF ABBREVIATIONS

ACC	Adaptive Cruise Control
ACF	After Lane Changing Car Following
ALC	Active Lane Changing
BCF	Before Lane Changing Car Following
CACC	Cooperative Adaptive Cruise Control
CF	Car Following
DLC	Discretionary Lane Change
GEH	Geoffrey E. Havers (GEH) Statistic
HOV	High Occupancy Vehicle
I2V	Infrastructure-to-Vehicle
LC	Lane Changing
ML	Managed Lane
MLC	Mandatory Lane Changing
O-D	Origin-Destination
RCF	Receiving Car Following
V2V	Vehicle-to-Vehicle
VAD	Vehicle Awareness Device
VMT	Vehicle Miles Traveled
VTT	Vehicle Time Traveled
YCF	Yielding Car Following

CHAPTER 1. INTRODUCTION

BACKGROUND

Cooperative Adaptive Cruise Control (CACC) is a term that has been used rather loosely in recent years, such that different people visualize different functions and capabilities when discussing CACC systems. Thus, there are now multiple system concepts that have been described under the CACC label, and the functionalities included in these varied concepts can be quite different from each other. At the heart of each CACC concept is the combination of Adaptive Cruise Control (ACC), a subset of the broader class of automated speed control systems, with a cooperative element, such as Vehicle-to-Vehicle (V2V) or Infrastructure-to-Vehicle (I2V) communication. The V2V communication provides information about the vehicle or vehicles directly ahead of the subject vehicle, and the I2V communication can provide information about traffic further ahead or about current speed restrictions as part of an active traffic management approach.

The primary motivation for the development of CACC is to improve highway and roadway capacity and throughput. The class of CACC systems utilizing V2V communication could allow the mean following time gap to be reduced from about 1.4 seconds when driving manually to on the order of 0.7 seconds when using CACC (Nowakowski, et al., 2010, and Nowakowski, O'Connell, Shladover, and Cody, 2010), resulting in an increase in highway lane capacity. Several California PATH highway traffic simulations (VanderWerf, et al., 2001, 2002, and Shladover et al., 2012) showed that ACC alone, even at high market penetrations, had little effect on lane capacity, and recent research (Milanés and Shladover, 2014) has even suggested that a stream of consecutive ACC vehicles would fail to achieve string stability, resulting in a negative impact on traffic capacity. However, with the shorter following gaps enabled by CACC systems, lane capacity could potentially be increased from the standard 2200 vehicles per hour to almost 4000 vehicles per hour at 100 percent market penetration.

PROBLEM STATEMENT

Despite the broad consensus that CACC has great potential for traffic improvement, there is still uncertainty regarding the impacts of CACC on the traffic flow dynamics. While an authoritative prediction of traffic impacts of CACC at various market penetrations is in great need, it is not feasible to determine the impacts by performing a large-scale field test before CACC is widely equipped in the vehicle fleet. Traffic micro simulation is a promising tool for exploring the influence of new technologies on traffic flow. But there is no existing simulation platform to capture the microscopic car following and lane changing behaviors of CACC vehicles and their interactions with manually driven vehicles. The existing simulation studies either analyze the CACC operation in a one-lane freeway, without considering the lateral interactions of vehicles (Shladover et al., 2012); or depict the car following and lane changing behaviors of both manually driven vehicles and CACC vehicles by using the same behavior model with different model parameter settings (van Arem et al., 2006). None of the existing simulation studies have adopted the realistic CACC vehicle behavior model developed in our previous study based on empirical data representing real-world CACC strings (Milanés et al., 2014). There is no existing research that performs the mobility analysis in a multilane freeway site, with specific modeling

of interactions among CACC vehicles and manually driven vehicles under various CACC operation strategies.

Achieving high-performance traffic streams with CACC requires not only robust vehicle control and communication systems, but also CACC operation strategies that help create CACC vehicle strings in the traffic stream and maintain the string operation. While the development of the control and communication systems has been reported in existing studies (Dey et al., 2016), there has been little research concerning the examination of CACC operation strategies or quantification of their impact on the highway capacity and throughput in a complicated multi-lane freeway environment. Without the operation strategies, CACC vehicles will mix randomly with manually driven vehicles in the traffic stream so that the formation of CACC strings is entirely determined by the random process. The existing strings can be easily interrupted because of the interactions among the manually driven vehicles and the CACC vehicles. The breakdown of the CACC vehicle strings might aggravate the traffic congestion at the freeway on-ramps and off-ramp bottlenecks. Because of the traffic disturbances caused by the merging and diverging traffic, the mainline CACC drivers may be forced to frequently turn off CACC and switch back to manual control. In the process, the drivers must decelerate to increase their car-following time gap, which could further intensify the traffic disturbances.

RESEARCH OBJECTIVE

To address the above problems, we have defined a twofold study objective. We aim to firstly provide a realistic estimation of the impacts of CACC on the freeway capacity and throughput. The second objective is to determine the CACC operation strategies that create the most capacity and throughput improvement on the freeway traffic stream. The research objective has been fulfilled through completing the following tasks:

1) Define CACC operation strategies that enhance the CACC string operation through an extensive literature review.
2) Build a microscopic traffic simulation model that realistically reproduces the behaviors of human drivers and their interactions with CACC vehicles.
3) Develop models that depict the CACC vehicle behaviors under various operation strategies and integrate the CACC models with the human driver model.
4) Model transportation networks where CACC could be implemented and calibrate the simulation models for these networks.
5) Perform analyses to quantify the impacts of CACC on the traffic flow in the identified networks and specify the recommended CACC operation strategies that bring about the best traffic impacts.

To fulfill the above tasks, both the PATH team and the TU Delft team have incorporated the CACC/ACC behavior model into their separate traffic simulation frameworks. The simulation experiments with similar initial conditions and parameter settings have been performed to identify the impact of CACC under various operation strategies. As we will see later in the report, the results from both team are consistent, indicating the credibility of our findings.

REPORT ORGANIZATION

The next section presents the CACC operation strategies identified from the literature review. Section 3 elaborates the human driver model and CACC vehicle behavior model. Section 4 includes the description of the road networks for analysis, and model calibration and validation results. In Section 5, we discuss the simulation results obtained from a simple freeway network study and the California State Route 99 corridor study. The conclusions and recommendation for future research are given in Section 6.

CHAPTER 2. CACC OPERATION CONCEPT ALTERNATIVES

A successful CACC operation strategy can increase the probability for individual CACC vehicles to join strings. Once a string is formed, the strategy can also help maintain the string operation throughout a highway corridor. Larson et al. (Larson, Krammer, Liang, and Johansson, 2013, and Larson, Liang, and Johasson, 2014) proposed a strategy that applies the high-level coordination and allows CACC vehicles to form strings at individual highway entrances based on their origin and destination. The strategy of (Liang, Mårtensson, and Johansson, 2013) aims to send acceleration or deceleration instructions to CACC vehicles in the traffic stream so that they can match with each other dynamically. Those strategies require coordination offered by traffic management centers or roadside units. They might not be implemented in the field until a substantial portion of the vehicle fleet adopts CACC. Before achieving the high-level coordination, we can also take advantage of existing highway facilities or modify the CACC control algorithms for better CACC string operation. For example, the implementation of the CACC managed lane can to some extent segregate the CACC traffic flow from the interruption of the manually driven vehicles. As CACC vehicles concentrate in the managed lane, they have a higher probability of forming strings. We can also encourage the application of Vehicle Awareness Devices (VAD) among manually driven vehicles. This strategy increases the probability that CACC vehicles operate in CACC strings because it allows a CACC vehicle to join a string led by a VAD vehicle (Shladover et al., 2012). Another potential strategy can use the on-board human-machine interfaces to change CACC drivers' discretionary lane change preferences such that they will stay in the string until they must exit the string to continue their routes. Since those strategies require little upgrade to the existing highway infrastructure, they might be implemented in the field as the CACC vehicles first emerge in the traffic stream.

In this study, we narrow our consideration to the impact analysis for strategies that are likely to be implemented soon, without requiring major upgrades of the existing road infrastructure. The evaluation of the high-level coordination strategies will be performed in our future research. The detailed literature review regarding the CACC operation concept alternatives can be found in a separate report entitled *Using Cooperative Adaptive Cruise Control (CACC) to Form High-Performance Vehicle Streams Definitions, Literature Review and Operational Concept*. The CACC operation strategies analyzed in this study are listed as follows:

- Implementation of Vehicle Awareness Devices (VAD) on manually driven vehicles. The VAD vehicles have the wireless communication capability. They can broadcast real-time information regarding their operation status and route choice. Although they don't have an automated controller to perform the car-following task, they can serve as the leader of CACC vehicle strings. With this strategy, the probability for CACC vehicles to travel in the CACC mode greatly increases. It thus offers incentives for users to equip with CACC, even when the CACC market penetration is low.
- Implementation of CACC managed lane (ML). The managed lane strategy has been widely used to serve high occupancy vehicles or drivers willing to pay a toll, with the purpose of improving the overall efficiency of the highway system. The CACC managed lane can adopt a similar operation concept that only allows CACC vehicles and VAD vehicles to enter the managed lane. It physically separates the CACC traffic stream and the regular traffic. As the CACC vehicles concentrate in the managed lane, they will have

a higher probability of traveling in CACC strings. The managed lane also reduces the interaction between the CACC vehicles and manually driven vehicles. The CACC strings are less likely to be interrupted in the managed lane.

- Discouraging discretionary lane changes for CACC string leaders and followers (DLC restriction). This strategy can be achieved by using an on-board device that offers real-time lane change guidance for drivers. When a driver is in a CACC string, we expect that her or his lane change behaviors will be different from what the driver would normally do, building on the existing experience of ACC drivers. Although there is no firm empirical data quantifying this behavior change, we can perform the what-if analysis to determine the outcomes if we offer the lane change guidance or restrictions to the CACC drivers. With this strategy, the drivers are encouraged to stay in the CACC string whenever possible. In this case, the disturbances caused by the CACC drivers' lane change maneuvers can be reduced. Subsequently, the CACC string will have a higher probability to operate in a stable state.

- Making drivers stay in the CACC mode when they cannot find a gap in the target lane. This strategy applies to CACC drivers when they try to make a lane change, but the current gap in the target lane is not acceptable. In this case, the driver will continue driving in the CACC mode, instead of turning off the CACC and manually accelerating or decelerating for gap searching. This strategy can reduce the probability that the CACC strings are broken down due to drivers' mode switches.

- Offering early lane change advisory message for drivers that want to exit the freeway. This strategy is expected to help improve the traffic flow for the freeway diverging areas under high CACC market penetration. As the traffic volume increases with the CACC market penetration, the traffic flow density will become high, which makes it more difficult to make lane changes toward the off-ramp. When the driver is close to the exit but still cannot merge into the off-ramp, she or he might make aggressive lane changes to force into the target lane, potentially causing great disturbances to the traffic flow. If the early lane change advisory message is provided, the driver can start making lane changes at a longer distance upstream from the exit. In this case, she or he will have a better chance to find an acceptable gap such that the driver does not have to force into the target lane. Reducing the aggressive lane change behaviors can stabilize the traffic flow, and subsequently lower the probability of breaking the operation of CACC vehicle strings.

CHAPTER 3. MICROSCOPIC TRAFFIC FLOW MODELING

In this chapter, we present an overview of the traffic flow models developed by the PATH and Delft teams. The PATH microscopic traffic model includes three major components: the vehicle dispatching model, human driver model and ACC/CACC model. The vehicle dispatching model determines how a modeled vehicle enters the simulation network and the distribution of vehicle types. The human driver model and ACC/CACC model specify the car following and lane changing behaviors of the human drivers and ACC/CACC equipped drivers, and their interactions. This chapter gives a brief overview of those models. The detailed description of the simulation model can be found in the separate report entitled *Using Cooperative Adaptive Cruise Control (CACC) to Form High-Performance Vehicle Streams: Microscopic Traffic Modeling.*

The ACC/CACC simulation models developed by the Delft team are embedded in a simulation package named MOTUS. MOTUS is a microscopic simulation framework with fundamental and extendable models for generating human-driven vehicles and reproducing their trajectories. The default vehicle generating model determines how vehicles are generated at the beginning of the simulated network and the human driver model defines the vehicles' longitudinal and lateral responses to surrounding vehicles under human drivers' control. The default vehicle generating model and human driver model are further adapted to the U.S. freeway traffic with a managed lane operation. The ACC/CACC algorithms are incorporated into the framework as automated vehicle controls executed by the on-board unit. The ACC/CACC models specify vehicles' longitudinal response under automated controls. They are delicately designed to realistically model the drivers' switch on and off decisions and behavior as the modeled CACC vehicles have interactions with the human drivers. The detailed description of the simulation model can be found in the separate report entitled *Microscopic Traffic Simulations with Cooperative Adaptive Cruise Control (CACC) Vehicles.*

VEHICLE DISPATCHING MODEL

PATH Approach

The vehicle dispatching model is intended to generate very high volumes of vehicles at the source section. This is essential for simulating CACC strings that have much shorter time gaps between consecutive vehicles than conventional manually driven vehicles. Once the input volume and the minimum headway are specified, the vehicle dispatching model can determine the arrival times of individual modeled vehicles. The time interval between two consecutive vehicles is a random number drawn from the shifted negative-exponential distribution.

In addition, the model will lead to a 'stable' (i.e., steady state equilibrium) traffic condition at the beginning of the simulated network. The generated traffic represents the traffic flow as the mixed fleet has traveled in a sufficiently long freeway segment without disturbance induced by the merging and departing traffic. To obtain stable input flow, a "holding" function is applied to release vehicles at the equilibrium position—a position where the subject vehicle has an acceleration of zero and speed equal to the desired speed. When a vehicle is generated in a lane, the vehicle type will be assigned based on the fleet composition (e.g., percentages of human driven vehicles, ACC vehicles and CACC vehicles) specified in the simulation inputs. The

destination of each individual vehicle is determined based on the user specified O-D table or turning percentage at individual intersections and interchanges.

In this project, we consider the operation of a CACC managed lane, which only serves CACC vehicles or manually driven vehicles equipped with VAD. If the CACC managed lane is activated, the vehicle dispatching model first assigns the CACC and VAD vehicles to the managed lane at the source section. If the managed lane cannot accommodate all the CACC and VAD vehicles, the remaining vehicles are released into the general-purpose lanes, with priority given to the lane immediately adjacent to the managed lane.

MOTUS Approach

MOTUS's vehicle generating model uses user-specified traffic demand to determine the average headway between consecutive vehicles to be released into the network. A random coefficient following the negative-exponential distribution is applied to the averaged headway to make it stochastic. When the traffic demand is large, it is possible that the available space in the source link is smaller than a new vehicle's desired distance (the product of the initial speed and the desired time gap). In this case, the vehicle will be put in a virtual queue and later be placed in the network as a queued vehicle. Otherwise, the vehicle will be put into the network as a free vehicle.

ACC/CACC vehicles are not different from human driven vehicles in the process of vehicle generation. The automation systems are assumed to be activated when vehicles are generated. ACC/CACC vehicles are generated individually depending on their own desired speed, desired time gap and the random arriving time. In this case, it may take times for these vehicles to enter the stable car-following mode and form an ACC/CACC string. A preliminary test suggests a 2-km section as the simulation warm up section to facilitate the formation of ACC/CACC strings.

HUMAN DRIVER MODEL

PATH Approach

Microscopic human driver car-following behavior and their interactions with the nearby vehicles determine the overall traffic pattern at the macroscopic level. The proposed human driver model intended to describe such driver interactions is built upon the basic framework of the NGSIM oversaturated flow model proposed by Yeo et al. (2008). Some important extensions and modifications were made to depict detailed car following and lane changing behaviors that were not represented in the original model. In the proposed model, a driver's car following and lane changing behaviors are partitioned into fundamental driving modes (or movement phases):

- *CF*: Regular car following mode
- *LC*: Lane change mode, which includes discretionary lane change (DLC), active lane change (ALC) and mandatory lane change (MLC)
- *ACF*: After lane changing car following mode (a driver temporarily adopts a short gap after a lane change maneuver)
- *BCF*: Before lane changing car following mode (a driver speeds up or slows down to align with an acceptable gap in the target lane)

- *RCF*: Receiving car following mode (a driver temporarily adopts a short gap after a vehicle from the adjacent lane merges in front)
- *YCF*: Yielding (cooperative) car following mode

As depicted by figure 1, at the beginning of each simulation update interval, a subject driver will determine the driving mode based on a set of car following and lane changing rules. Each driving mode is associated with specific car following and lane changing algorithms, which are used to determine the driver's speed and position at the end of the update interval. Such an update process is executed iteratively for every modeled vehicle in the simulation environment, resulting in a trajectory for each vehicle over the simulation period. The detailed car following and lane changing algorithms are described in our report entitled "*Using Cooperative Adaptive Cruise Control (CACC) to Form High-Performance Vehicle Streams—Microscopic Traffic Modeling*".
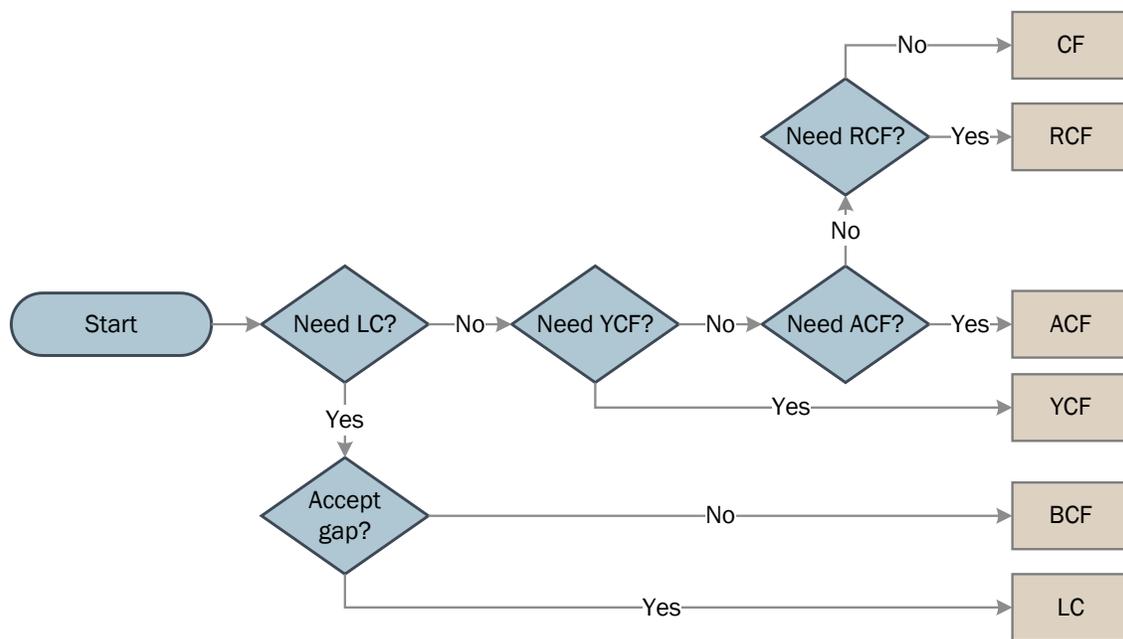
Figure 1. Flow Chart. Human driver model structure. This figure shows the simulation flow for modeling the behaviors of human drivers. The simulation algorithm first determines if a modeled driver needs to make a lane change. If the driver desires a lane change, the algorithm will determine if the current gap in the target lane is acceptable. When the gap is acceptable, the LC mode will be used to update the driver's behavior; otherwise the BCF mode will be implemented. When the driver does not need to make a lane change, the algorithm further checks if she or he is required to yield to another driver. The YCF mode will be used if the yielding behavior is demanded. When there is no need for yielding, the algorithm then determines if the ACF mode is necessary. If it is not, then the RCF mode is checked. The CF mode will be used if RCF is not required.

MOTUS Approach

The car following model for human drivers in MOTUS is a modified version of the Intelligent Driver Model by Treiber, Hennecke and Helbing (2000), hereinafter referred as IDM+ (Schakel, van Arem & Netten, 2010). The IDM+ provides the desired acceleration as the minimum of the acceleration of driving towards the desired speed and the acceleration towards the desired headway. This model has been proved to be capable of reproducing crucial traffic phenomena such as capacity drop (Kesting, Treiber & Helbing, 2010).

A Lane Change model with Relaxation and Synchronization (LMRS) introduced by Schakel, Knoop and van Arem (2012) is used in MOTUS to model the vehicles' lateral interactions and response. The LMRS model describes the lane change desires by a combination of three types of incentive: following the route, gaining speeds, and optional lane preference. The route and speed incentives work for most of the traffic situations while the lane preference incentive works in particular scenarios such as the dedicated lane scenario.

A decision model is used to determine a driver's lane change behavior based on the driver's lane change desires and a condition-dependent acceptable gap relaxation. Based on the total lane change desire, four different types of lane change behavior can be distinguished by three thresholds: d_{free}, d_{sync} and d_{coop}. As shown in Figure 2, if the total lane change desire d is smaller than d_{free}, no lane change (No LC) will be performed. When d is between d_{free} and d_{sync}, vehicles will execute free lane changes (FLC). When d is within the range of [d_{sync} d_{coop}], the lane changing vehicle will perform synchronized lane changes (SLC) where it aligns speed with that of the leader in the target lane, but the follower in the target lane does not actively create a gap for the lane changer. As the desire d exceeds d_{coop}, cooperative lane changes (CLC) are expected, in which the lane changing vehicle synchronizes its speed with the potential leader in the target lane and the potential follower in the target lane actively creates a gap in front to facilitate the lane change. The green line and red line in Figure 2 show the relaxations of the acceptable gap and acceptable deceleration for performing a lane change. As the lane change desire rises, lane changing vehicles accept smaller gaps and potential followers in the target lane allow larger deceleration for a cooperative lane change.
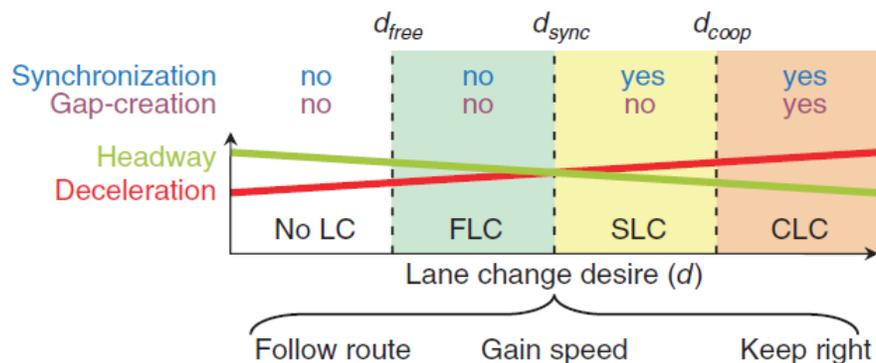
Figure 2. Graph. Four types of lane change behavior corresponding to the level of lane change desire (Schakel, Knoop et al., 2012). The figure shows the relationships between lane change desire and lane change behavior. The total desire is divided into four levels by the criteria

d$_{free}$, d$_{sync}$ and d$_{coop}$, and four lane change behavior are determined accordingly as No Lane Change, Free Lane Change, Synchronized Lane Change and Cooperative Lane Change. The lane changing vehicle with Synchronized Lane Change performs speed synchronization with the target vehicle in order to better find a cut-in gap, while only the Cooperative Lane Change strategy requests the potential follower of the lane changing vehicle for the courtesy gap creation. Besides that, the relaxations in the acceptable gap and the gap-creation decelerations are illustrated as two lines in the figure. The acceptable gap decreases with rising lane change desires but the acceptable deceleration for a potential follower increases when lane change desires grow.

ACC AND CACC VEHICLE BEHAVIOR MODEL

PATH Approach

We adopted the models developed in Milanes and Shladover (2014) to depict the ACC and CACC car following behaviors. CACC equipped vehicles exhibit significantly different car following behavior from manual drivers and can form strings that allow them to follow the preceding vehicles with short gaps. Drivers of CACC equipped vehicles can also exit their closely coupled string and switch off CACC to make lane changes or exit the freeway. The lane changing behaviors of the C/ACC drivers are depicted by the proposed C/ACC vehicle behavior model. The modelling framework of CACC vehicles is highlighted in figure 3. Although the CACC system implementation relies on information received from the leading vehicle in the CACC string as well as from the immediately preceding vehicle, the empirical models used in the simulation provide a simplified description of the closed-loop vehicle-following dynamics that are achieved relative to the immediately preceding vehicle. The simplified approach is suitable for modeling a large number of CACC vehicles.
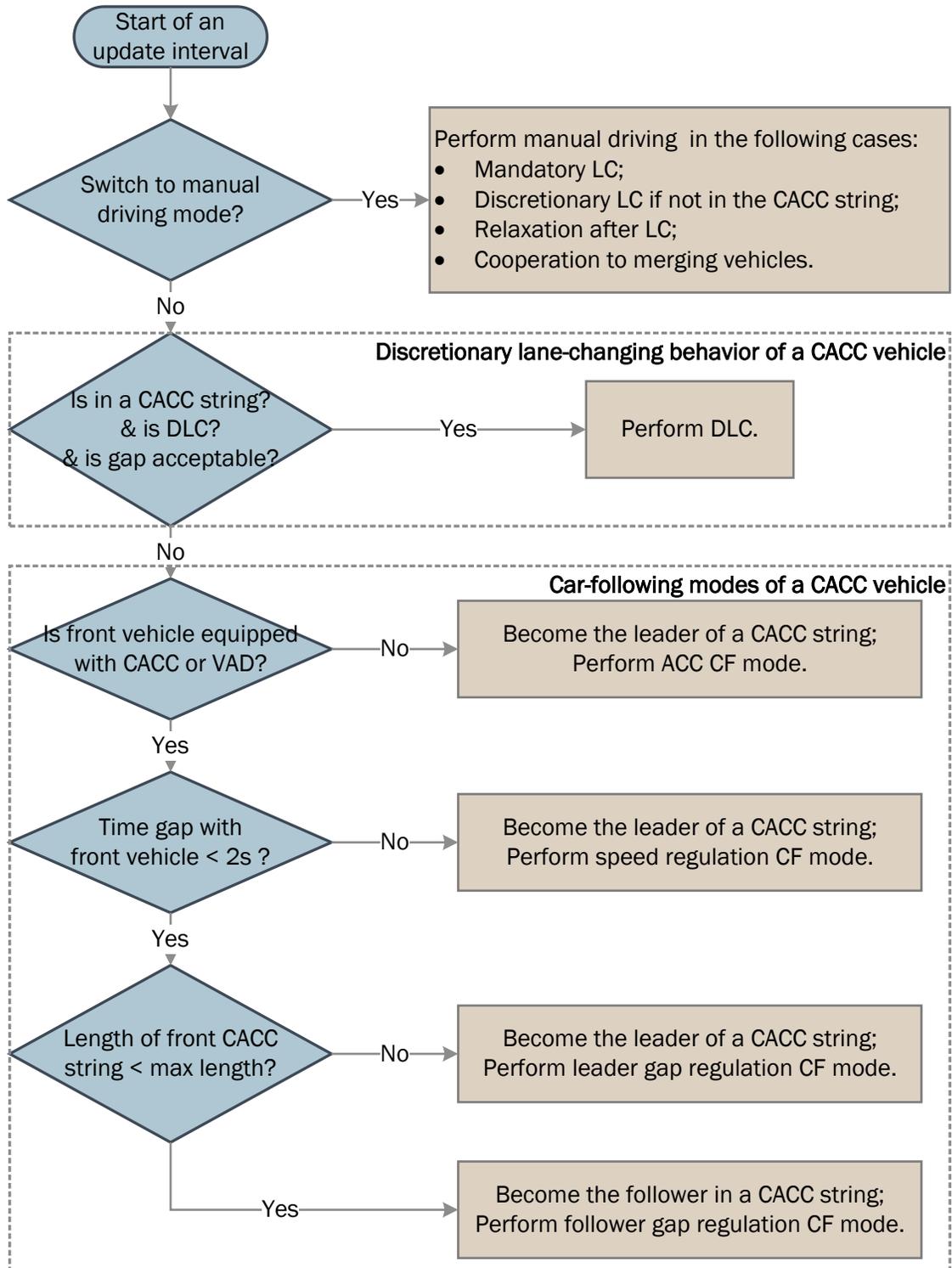
Figure 3. Flow Chart. Car following and lane changing dynamics of CACC vehicles. The figure demonstrates the simulation flow for CACC vehicles. The simulation algorithm first decides if the modeled CACC vehicle needs to make a lane change. If the lane change is desired, the algorithm will switch to the manual driving mode to model the target vehicle. Otherwise, the

algorithm will identify if the modeled vehicle is a CACC string leader or follower. The CACC vehicle is the string leader, if the preceding vehicle is not a CACC vehicle or VAD vehicle, or the time gap from the preceding vehicle is larger than 2 seconds, or the preceding CACC string reaches the maximum string length. Otherwise, the CACC vehicle is a string follower.

MOTUS Approach

The MOTUS model uses the same ACC/CACC algorithms adopted by the PATH model. When the ACC/CACC system is activated, the ACC/CACC algorithms substitute for the IDM+ and work as car-following models for each individual ACC/CACC vehicle.

A multi-regime model for ACC/CACC longitudinal vehicle response is proposed based on the two parallel control loops shown in Figure 4. The two parallel control loops are the human driver control loop and the system control loop. Each loop represents the sequential procedures for corresponding vehicle control within a simulated time step and both loops are based on a three-stage control structure from Milanes and Shladover (2012). The vehicle information received from the perception stage is processed either by ACC/CACC or human driver response models and eventually the actual kinematic data becomes model outputs and provides feedback information for the next time step.

The driver intervention and the collision warning system determine when to switch between the two control loops. They correspond to two types of authority transition: discretionary overrides and mandatory overrides. The discretionary override is initiated by drivers, for drivers actively interacting with the automation system. The mandatory override is activated as a collision warning is given in a safety-critical situation. Regarding automation activation, we assume the switch is only effective from the driver control loop to system control loop, and the automation system cannot switch on by itself.
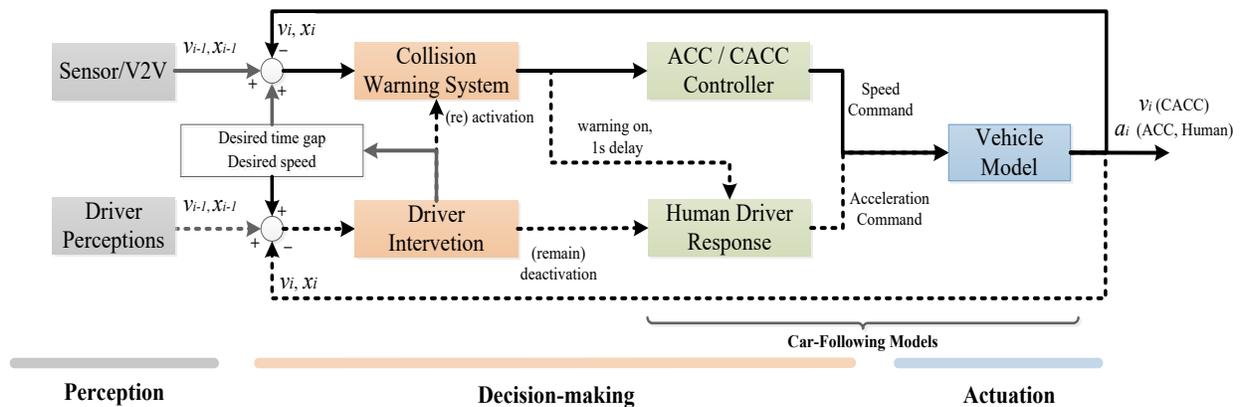
Figure 4. Graph. Conceptual longitudinal models for ACC/CACC vehicles in simulations. This figure illustrates a comceptual control framework combining both automated system controls and human driver controls. The automated system control and human driver control are two parallel control loops, going through the perception, decision-making and actuation stage. The sutomated system control receives the surrounding vehicle information from either sensors or V2V communication, and that information is used for the collsion warning system to idenfity the safety-critical situation. If a collision warning is not issued, the ACC/CACC controller

generates the speed/acceleration commands, which are inputs for the vehicle model in the actuation stage. The outputs of the vehicle model are the actual vehicle speed and acceleration and they are used in the next control interval, where a feedback control is formed. Similarly, the human driver control receives information from the driver's perceptions and a decision about interacting with the automated system control loop is made in the decision-making stage. Once the automation is deactivated or a collision warning is issued, the human driver model takes over and generates the acceleration command to the vehicle model. In the same way, the outputs are used for the next control interval for both control loops.

COMPARISON OF PATH MODEL AND MOTUS MODEL

To obtain comparable results from the two models, both the PATH model and the MOTUS model select the same ACC/CACC car-following model and make the simulation assumptions as close to each other as possible. Particularly, the same free cruising and car-following models of ACC/CACC vehicles are used in both simulators. This leads to similar ACC/CACC vehicle movements in equilibrium status. In addition, a similar simulation scheme with a collision warning system and human driver take-over algorithm is adopted by both models. In safety-critical situations, both PATH and MOTUS model switch from ACC/CACC controls to human driver controls based on collision warnings and collision-free simulations are thereby guaranteed. Besides that, the simulation is set up with consistent inputs, such as acceleration capability and sensor range in vehicle settings, desired ACC/CACC inter-string and intra-string time gaps in ACC/CACC system inputs, and a 10-vehicle limit on the vehicle string length in string operational settings.

There are also some differences between the two models. The PATH and MOTUS models made different assumptions in defining the ACC/CACC vehicle behavior in the approaching scenario and low speed scenario, where the actual vehicle responses have not yet been tested in the field. In the approaching scenario, the PATH model applies a hysteresis control to describe the transition between the free cruising mode and car-following mode; while MOTUS uses the base CACC car-following model with adjusted control gains. In the low speed scenario, the PATH model uses a 2-meter spacing as the minimum and the MOTUS model introduces a dynamic spacing margin varying with the vehicle's speed to prevent the collision. These discrepancies in ACC/CACC vehicle models result in slightly different vehicle responses and may lead to different vehicle trajectories. In addition, the PATH and MOTUS collision avoidance modules are based on two different algorithms. The PATH model estimates the potential collision 20 seconds in advance based on vehicle kinematics. In contrast, the MOTUS model adopts the possibility indicator developed by Kiefer, LeBlanc and Flannagan (2005) to estimate the safety-critical situation. The dissimilar collision estimation can lead to different timing to override the system. Finally, the PATH and MOTUS models provide different string join strategies. The PATH model allows a following string to join its preceding string even if the resulting new string will be longer than the string length limit. The string split process will then be executed to reduce the length of the new string. In MOTUS, however, the second string joins the first string only when the length of the new string is below the string length limit. With this difference, the PATH model encourages "full-length" strings while the MOTUS model reserves more inter-string gaps in the traffic stream.

CHAPTER 4. HUMAN DRIVER MODEL CALIBRATION

The human driver models from PATH and MOTUS were first calibrated against ground truth data before analyzing the impacts of ACC/CACC vehicles. The model calibrations provide solid evidence and support for simulated vehicle behavior and traffic flow, offer a benchmark for ACC/CACC vehicle impact analysis, and build up a connection between the PATH and MOTUS models for comparable results.

The SR99 corridor to the south of Sacramento, California, is selected as the calibrated network. The network starts from the on-ramp of Elk Grove to the off-ramp toward SR50, with 20 km in length, 16 on-ramps and 12 off-ramps (See Figure 5 for lane configuration). The considered time period is from 4:00 AM to 12:00 PM. Loop detector data in this corridor were obtained from the Caltrans Performance Measurement System (PeMS), which provides 5-mins flow and speed data for each lane on the mainline of the corridor. We chose the date of October 6, 2015 - a typical weekday without incident reports during the selected time period. Unreliable data violating the principle of vehicle conservation were removed, resulting in 16 reliable groups of mainline detectors for demand imputation and calibration.
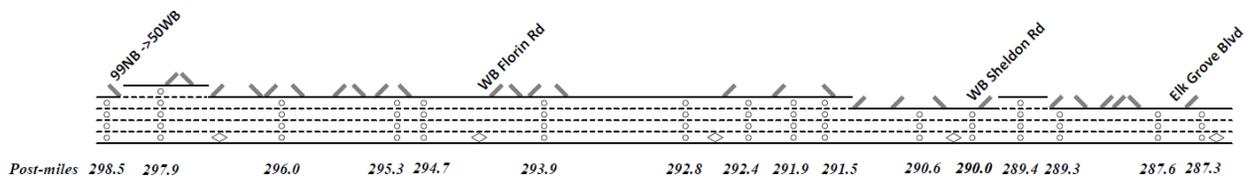
Lane configuration and road geometry
Figure 5. Graph. Study site: SR-99 freeway south of downtown Sacramento, CA. This figure depicts the road configuration of the SR-99 freeway corridor, starting from Elk Grove Blvd to the interchange to SR-50 WB. There are 16 groups of detectors, from the south to north, the mileposts are 287.3, 287.6, 289.3, 289.4, 290.0, 290.7, 291.5, 291.9, 292.4, 292.8, 294.0, 294.7, 295.3, 296.0, 297.9 and 298.5. The WB Florin Rd and WB Sheldon Rd were denoted in the figure as the on-ramp bottlenecks.

The SR99 Corridor has a median exclusive HOV lane with continuous access and egress operating only from 6:00 AM to10:00 AM. Data from both free-flow and congested-flow can be obtained due to recurrent congestion, providing sufficient data for model calibration. The empirical data reveal a complex congestion pattern with interacting bottlenecks in the morning peak. Propagation and recovery of the congestion can also be recognized.

MODEL GOODNESS-OF-FIT INDICATOR

Multiple replications of the simulation model run with different random number seeds were made in order to calibrate the models to the conditions of October 6, 2015. The predicted flows and speeds at selected locations on the freeway were compared with real traffic measurements at every 5-minute interval to assess the accuracy of the simulation models in representing the observed conditions. The model goodness-of-fit is measured by two indicators: GEH and Mean-Absolute-Percentage-Errors (MAPE).
        The GEH statistic is computed as

$$GEH(k) = \sqrt{\frac{2[M(k) - C(k)]^2}{M(k) + C(k)}} \qquad (3)$$

where,

$M(k)$: simulated flow during the k-th time interval (veh/hour)
$C(k)$: flow measured in the field during the k-th time interval (veh/hour)

and the MAPEs of flows is defined by equation 4.

$$MAPE = \frac{1}{N \cdot T} \sum_{n=1}^{N} \sum_{t=1}^{T} \frac{M_{n,t}^{real} - M_{n,t}^{sim}}{M_{n,t}^{real}} \qquad (4)$$

N is the number of detectors and T is the number of time intervals. $M_{n,t}^{real}$ and $M_{n,t}^{sim}$ are the field observed and simulated data (i.e. flow) of detector n obtained during time interval t, respectively.

The simulated flow is acceptable based on: (1) on average of all detectors, for at least 85% of all 5-minute time intervals, the flow is to satisfy the condition that $GEH(k) < 5$ and (2) the MAPE must be less than 10%.

Above all, the simulated flow-density relationship and queue propagation must be visually acceptable. This indicates that the fundamental diagrams of field observed and simulated flow vs. density should resemble similar patterns for key bottlenecks along the corridor, and the contour plots of the field observed and simulated speeds at all 5-minute intervals should exhibit similar trends over the length of the corridor as well as the duration of the study period.

CALIBRATION METHODS AND PROCEDURES

PATH Model Calibration

Parameters in the model were adjusted by a few iterations of trial and error to find the best fit for the given field data. More sophisticated algorithms were avoided in order to ensure reasonable simulation and computation time for this complex corridor. Simulation experiments suggest that the following parameters provide a good fit:

- Reaction time (τ_r): 0.8 s
- Maximum acceleration (a_M): 2.0 m/s^2
- Maximum deceleration (b_f): 4.0 m/s^2
- Time headway (τ_h): 1.40 s
- Coefficient of lane friction (c_f): 0.5
- Speed difference threshold for DLC $\left(\frac{v_{ant} - \tilde{v}_0}{\max(\tilde{v}_0, V_{dlc})}\right)$: 0.15

However, poor visibility near on-ramp merging areas on the upstream 2-mile section of the corridor required increasing the reaction time to 1.0 s to better reproduce the field observations.

Furthermore, frequent aggressive and last-minute lane changes observed in the field required reducing the reaction time to 0.4s for the short weaving section between the upstream 12th Ave. on-ramp and the downstream US-50 off-ramp in order to replicate the high capacity and relatively uncongested off-ramp bottleneck near the US-50 freeway interchange. More than half of the SR-99 traffic makes lane changes to access the US-50 off-ramp during the morning peak.

MOTUS Model Calibration

In the MOTUS platform, the to-be-calibrated parameters involve both the lane change model LMRS and the car-following model IDM+. The calibration starts from the free-flow scenario where parameters corresponding to free driving behavior are determined. The set of parameters with minimum values of the objective function was selected as the calibrated parameters for free flow conditions. Next, the parameters were calibrated in congested conditions. Following the procedures in the previous stage, a sensitivity analysis of the results with varying parameter values was conducted to narrow down the range of each parameter. Then we checked the congestion pattern before the quantitative analysis of GEH and MAPE of flow and searched the parameter values by plausible congestion pattern with acceptable errors. The calibrated parameters are shown in TABLE 1.

Table 1. Calibrated MOTUS parameters of the SR99 corridor.

Parameter/Symbol	Original values	Calibrated values
Sensitivity to speed gain / v_{gain}	69.6 km/h	54 km/h
Car acceleration/ a_{car}	1.25 m/s^2	1.25 m/s^2
Free lane change criteria/ d_{free}	0.365	0.25
Synchronized lane change criteria/ d_{sync}	0.577	0.5
Cooperative lane change criteria/ d_{coop}	0.788	0.75
Maximum deceleration/ b	2.09 m/s^2	2.09 m/s^2
Average maximum headway/T_{max}	1.2 s	1.4 s
Average minimum headway/T_{min}	0.56 s	0.52 s
Lane change desire per lane/ t_0	43 s	52 s
Averaged free-flow speed/ $V_{des,car}$	123.7 km/h	125 km/h
σ_{car}	12 km/h	8.75 km/h
HOV bias/ d_{HOV}	-	0.45
SOV bias/ d_b	-	0.5
Low desire-speed bias	-	0.25
Local high desire-speed bias	-	0.25

MODEL COMPARISON AND DISCUSSION

Quantitative Results

TABLE 2 summarizes the flow calibration results for the 16 detectors that provided good data along the 13-mile stretch of northbound SR-99. The HOV lane data were aggregated with those of the general-purpose lanes because the HOV lane is equally congested and exhibits nearly the same congestion pattern (bottleneck location and duration) as the general-purpose lanes. It can be seen that on average, the simulated flows satisfied the calibration criteria. However, the PATH model

cannot accurately simulate the flow of the downstream weaving bottleneck at US-50, under both the GEH and MAPE criteria. This could be attributed to the limitation that that model's lane changing logic does not reflect the unusually aggressive and frequent lane change behavior. Modeling such an area may require better developed lane changing gap acceptance criteria that specifically fit such an off-ramp bottleneck.

The MOTUS model met the GEH criterion at all the detector stations along the whole corridor. Although the overall MAPE were less than 10%, the MAPE at 4 locations (out of 16 detector stations) were slightly higher than 10%. These correspond to the Elk Grove bottleneck, EB Sheldon bottleneck and the EB Mack bottleneck, where throughput during congestion is lower in simulation than that in the field.

Table 2. Calibration of freeway flows.

Freeway: 5-min flows of SR-99 Northbound						
Criterion 1: GEH						
Detector Location (post-mile)	Target	PATH		MOTUS		
		% Met	Target Met?	% Met	Target Met?	
287.3	GEH < 5 for > 85% of k	100%	Yes	94.67%	Yes	
287.6	GEH < 5 for > 85% of k	97.92%	Yes	91.78%	Yes	
289.3	GEH < 5 for > 85% of k	98.65%	No	93.78%	Yes	
289.4	GEH < 5 for > 85% of k	98.54%	Yes	94.44%	Yes	
290.0	GEH < 5 for > 85% of k	98.65%	Yes	95.56%	Yes	
290.7	GEH < 5 for > 85% of k	97.71%	Yes	96.44%	Yes	
291.5	GEH < 5 for > 85% of k	93.54%	Yes	95.11%	Yes	
291.9	GEH < 5 for > 85% of k	91.04%	Yes	92.67%	Yes	
292.4	GEH < 5 for > 85% of k	93.23%	Yes	92.00%	Yes	
292.8	GEH < 5 for > 85% of k	93.13%	Yes	92.22%	Yes	
294.0	GEH < 5 for > 85% of k	92.81%	Yes	95.11%	Yes	
294.7	GEH < 5 for > 85% of k	94.79%	Yes	94.22%	Yes	
295.3	GEH < 5 for > 85% of k	94.90%	Yes	95.78%	Yes	
296.0	GEH < 5 for > 85% of k	88.65%	Yes	99.56%	Yes	
297.9	GEH < 5 for > 85% of k	79.27%	No	98.67%	Yes	
298.5	GEH < 5 for > 85% of k	92.50%	Yes	98.44%	Yes	
Overall	GEH < 5 for > 85% of k	94.08%	Yes	95.03%	Yes	
Criterion 2: MAPE						
Detector Location (post-mile)	Target	PATH		MOTUS		
		% Met	Target Met?	% Met	Target Met?	
287.3	MAPE < 10%	1.99%	Yes	5.58%	Yes	
287.6	MAPE < 10%	9.36%	Yes	11.85%	No	
289.3	MAPE < 10%	9.17%	No	10.80%	No	
289.4	MAPE < 10%	8.61%	Yes	9.88%	Yes	
290.0	MAPE < 10%	6.85%	Yes	8.42%	Yes	
290.7	MAPE < 10%	7.41%	Yes	9.08%	Yes	
291.5	MAPE < 10%	9.92%	Yes	10.56%	No	
291.9	MAPE < 10%	10.38%	No	11.21%	No	
292.4	MAPE < 10%	8.98%	Yes	9.59%	Yes	
292.8	MAPE < 10%	8.02%	Yes	9.35%	Yes	

294.0	MAPE < 10%	8.37%	Yes	9.01%	Yes
294.7	MAPE < 10%	7.37%	Yes	8.26%	Yes
295.3	MAPE < 10%	8.01%	Yes	8.14%	Yes
296.0	MAPE < 10%	10.52%	No	7.48%	Yes
297.9	MAPE < 10%	14.20%	No	7.23%	Yes
298.5	MAPE < 10%	14.09%	No	8.49%	Yes
Overall	MAPE < 10%	8.21%	Yes	9.06%	Yes

Flow Characteristics Comparison

FIGURE 6 summarizes the simulated vs. observed queue propagation. The contour plots show the 5-minute average speeds at the detectors throughout the selected peak period. The first and last hour (low demand and free-flowing) were omitted from the figures. Both models reproduced the field observed peak duration and the length of queue fairly accurately, with the exception of the most upstream bottleneck at Sheldon Rd., which the PATH model simulated with slightly shorter congestion duration and slightly less queue propagation. Additionally, the PATH model simulated faster queue dissipation, as evident in the shorter peak duration shown in FIGURE 5(b). This could be attributed to the higher acceleration and deceleration rate applied in the PATH model. The lane changing and gap acceptance criteria required larger acceleration and deceleration to prevent simulating low bottleneck flows and severe queue propagation. This compromised the accuracy of peak duration but can be fixed with systematic optimization instead of trial and error to search for the best set of parameters.

The PATH model was able to replicate the speed profiles of the most downstream bottleneck, which is a complex weaving section with more than 50% off-ramp traffic. In MOTUS, a special local headway was applied here to meet the traffic throughputs but unfortunately the model could not simulate the slight speed reduction at this bottleneck.

(a) field observation	**(b) PATH simulation**	**(c) MOTUS simulation**
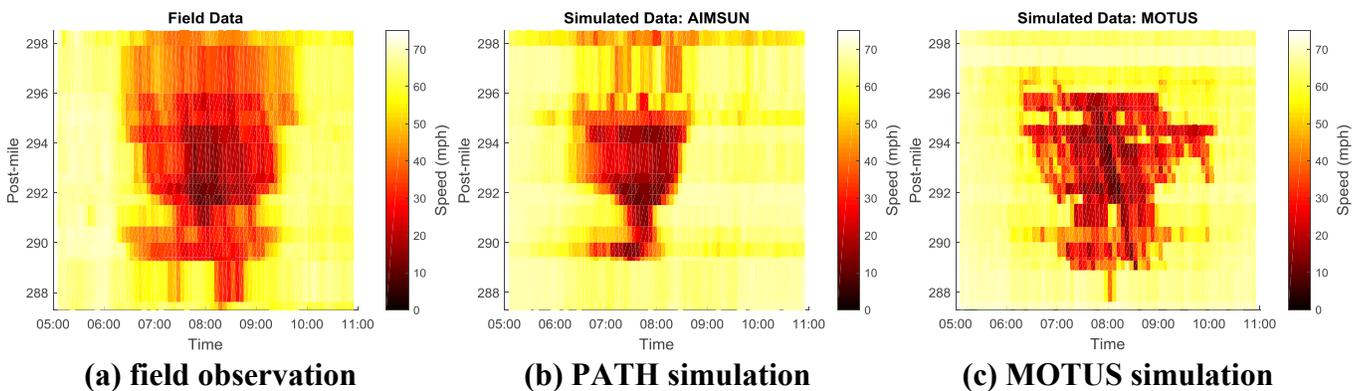
Figure 6. Graph. Comparison of speed contour plots between field observation, PATH simulation and MOTUS simulation. Three sub-figures of speed contour plots are presented here for the comparison of traffic congestion pattern. The left sub-figure (a) shows the congestion pattern from the ground-truth data that congestions almost covered the whole network within the peak hours and congestion propagation and dissolution are observed. The middle sub-figure (b) shows the PATH simulation results that the upstream bottleneck is less congested without propagation and the congestions are dissolved sooner than the ground-truth data. The right sub-figure (c) shows the MOTUS simulation results that no congestion appears at the

18

downstream network after PM 296 and the congestions last longer till 10:00 AM. Other than that, the formation and propagation of the traffic congestion are captured by both simulation models and the congestion intensity is also accurately reproduced.

CHAPTER 5. IMPACT OF CACC OPERATION ON TRAFFIC FLOW

SIMULATION SETUPS

A virtual simplified network is first established in order to better show the ACC/CACC impacts without possible interference and consequences resulting from interacting bottlenecks in the realistic network. The simplified network is a simple 4-lane freeway segment with an on-ramp and an off-ramp (see figure 7). The freeway mainline is 7 kilometers long. The source links in the network are highlighted by the red boxes. The simulated vehicles are released into the network through the source links. There is a 2-kilometer 'warm-up' mainline segment immediately downstream from the mainline source link. The simulated vehicles will use this segment to reach a stable car-following state after entering the network. This segment also allows CACC vehicles to form stable CACC vehicle strings in the CACC analysis cases.
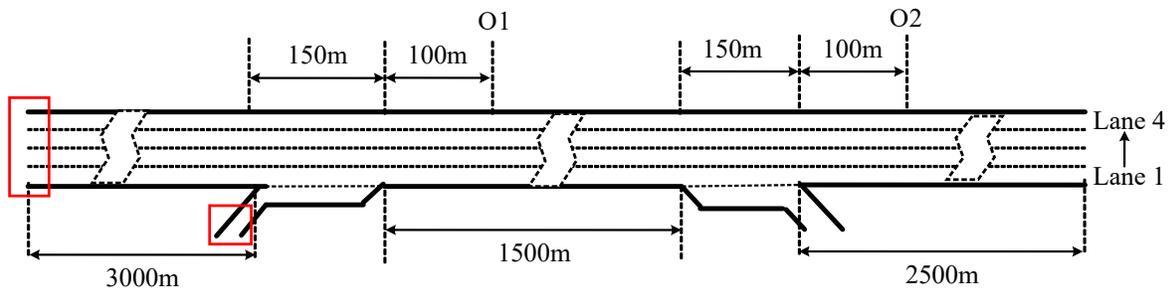
Figure 7. Illustration. Sketch plot of simple network. This figure depicts the simple simulation network. The network contains a 7-kilometer freeway segment with 4 mainstream lanes. There is an on-ramp 3 kilometers downstream from the beginning of the network. An off-ramp is located 4.65 kilometers from the network beginning. Both the on-ramp acceleration lane and off-ramp auxiliary lane are 150 meters long. There are two data collection locations. The first location O1 is 100 meters downstream from the end of the on-ramp; and the second location O2 is 100 meters downstream from the end of the off-ramp. The rightmost lane is Lane 1 and leftmost lane is Lane 4.

The MOTUS simulation uses a similar simplified network as that in figure 7 with some minor differences. Instead of 7 kilometers in length, the simplified network in the MOTUS simulation is 11 kilometers long with the same configuration of one on-ramp and one off-ramp. The auxiliary lanes for the ramps are defined as 250 meters, which works better with the MOTUS lane change model and better facilitates the merging process. The detectors are placed at 200 meters downstream of the merging/diverging sections, which are denoted as O1 and O2 in figure 7.

Our analysis started with the identification of the pipeline capacity of the simple network. Results of the analysis could reveal the impact of the CACC string operation on the basic freeway segment. To this end, we specified a zero on-ramp and off-ramp traffic flow and then measured the traffic flow of the four-lane freeway network under various CACC market penetrations. The pipeline capacity was defined as the maximum 15-minute moving average flow rate observed in the middle of the network, according to the Highway Capacity Manual

(HCM, 2010). The experiments began with simulating a constant and relatively low traffic volume for one hour. If the freeway remained free-flowing, then subsequent simulations were conducted with slightly higher volume input (e.g., plus 1000 veh/hr), until the highest observed 15-minute moving average flow no longer increased as the input became larger. The capacity was finally determined based on five replications with different random seeds. These procedures were simulated for 0%, 20%, 40%, 60%, 80%, and 100% market penetration of CACC equipped vehicles.

The next study concerned the performance of the freeway merge bottleneck under various CACC market penetrations. The on-ramp merging area depicted in figure 7 was used for the study. In the analysis, we fixed the freeway mainline traffic input at the pipeline capacity measured under different CACC market penetration cases in the previous study. The on-ramp traffic volume increased from 300 veh/hr to 1500 veh/hr, with a 300 veh/hr increment. In each simulation run, the mainline traffic was first released for 20 minutes. Afterwards, the on-ramp traffic was loaded together with the mainline traffic for 40 minutes. In the last 10 minutes of the simulation, both upstream mainline and on-ramp traffic volume were set to zero. The vehicles remaining in the network could leave the simulated freeway in that period. The freeway throughput was observed at the location O1 as shown in figure 7. In the analysis, we only used the traffic data collected in the last 30 minutes of the 40-minue period when the on-ramp traffic was loaded. The first 10-minute data were eliminated because the traffic flow may experience fluctuations and/or breakdown as the on-ramp traffic first entered the freeway mainline. Such a flow fluctuation can lead to an unstable queue discharging flow. The 15-minute moving average flow rate was computed based on the 30-minute data. The maximum 15-minute flow rate was considered as the throughput of the merging area.

The last study with the simple network was performed at the off-ramp diverging area depicted in figure 7. The study revealed the percentage of the mainline traffic that could exit the freeway without causing traffic breakdown. In the analysis, we made the mainline traffic input equal to the pipeline capacity for each CACC market penetration. The off-ramp traffic was initially set as 5% of the mainline flow. Additional simulation runs were performed for the off-ramp traffic percentages of 10%, 15%, 20% and 25% as well. The traffic flow was measured at the location O2 as shown in figure 7. The simulation time was 1 hour and the data of the last 40 minutes were used to compute the 15-minute moving average flow rate. The highest 15-minute moving average flow rate was considered as the throughput downstream of the diverging bottleneck.

The impact of the CACC operation strategies on the capacity and throughput improvement was also discussed for the pipeline, on-ramp bottleneck, and off-ramp bottleneck cases. The analysis processes mentioned above were performed with and without the higher-level operation strategies. Particularly, the ML strategy was only tested for the 40%, 60%, and 80% CACC market penetration cases. In the 20% penetration case, the CACC vehicles in the fleet were not enough to exclusively occupy a lane. The VAD strategy was tested for cases with 20%, 40%, 60% and 80% CACC market penetration. The DLC restriction strategy was analyzed in all CACC cases. The lane change advisory strategy was applied in the off-ramp analysis only.

The traffic flow dynamics of the SR-99 corridor were compared under 0%, 20%, 40%, 60%, 80% and 100% CACC market penetrations. Under the low CACC market penetrations, we also examined the differences with and without the VAD and ML strategies. The traffic demand input

was obtained from the field observations and it was the same for all the scenarios. The simulation period was an 8-hour period from 4:00 am to 12:00 pm. The total vehicle miles traveled (VMT), total vehicle time traveled (VTT), and average space mean speed were used for measuring the mobility performance of each scenario. To compute the average space mean speed, the space mean speed of the entire corridor was observed every 5 minutes in a simulation run. The measured speed data were the basis to compute the average speed. There were 5 simulation replications for each scenario. The performance measures were estimated based on the averaged data across those replications.

DETERMINATION OF MAXIMUM CACC STRING LENGTH AND INTER-STRING TIME GAP

We have identified the maximum CACC vehicle string length and the inter-string time gap to be implemented in the CACC string operation. These parameters are particularly important for achieving good traffic performance at on-ramp and off-ramp areas where the merging or exiting vehicles make frequent mandatory lane changes. With suitable levels for the two parameters, we can achieve both significant improvement of the freeway capacity and throughput, and stable traffic flow where the merging and exiting vehicles can easily find acceptable gaps in the target lane to merge into, without causing severe disturbances.

The analysis was performed in the simple network under 100% CACC market penetration. The on-ramp and off-ramp traffic volumes were fixed at 500 veh/hr each. The tested levels of the maximum string length were 5, 10, 15, 20, and 25 vehicles; and the inter-string time gaps were 1.0, 1.5, 2.0 and 2.5 seconds. The experiments began with simulating a constant and relatively low mainline traffic volume for one hour. If the freeway remained free-flowing, then subsequent simulations were conducted with slightly higher volume inputs (e.g., plus 1000 veh/hr), until the highest observed 15-minute moving average flow no longer increased as the input became larger. Then we measured the maximum 15-minute throughput at both the on-ramp and off-ramp area (locations O1 and O2 in Figure 1) as the performance metrics.

The freeway throughput at the on-ramp and off-ramp location is listed in Tables 3 and 4. When the inter-string gap is 1.0 second, the freeway throughput increases with the maximum string length as the maximum length is 15 vehicles or less. When the maximum length becomes higher, it becomes more difficult for the merging and diverging vehicles to find acceptable gaps in the target lane. In this case, those vehicles have to make aggressive lane changes, thus creating traffic disturbances that lead to traffic breakdown. Under this traffic condition, the throughput declines as the maximum string length increases. When the inter-string gap is 1.5 seconds or longer, the throughput reduces linearly with the inter-string time gap at both the on-ramp and off-ramp site. On the other hand, the throughput increases with the string length, although the increase becomes smaller after the string length is longer than 15. The throughput increase does not have a linear pattern with the string length because longer strings can negatively impact the traffic operation at the on-ramp and off-ramp sections. Such a negative impact offsets the throughput increase that could have been achieved with longer strings.

Table 3. Freeway throughput (veh/hr/ln) at the on-ramp area under various maximum CACC string length and inter-string time gap levels.

Max string length	Inter-string time gap (s)			
	1.0	1.5	2.0	2.5
5	3105	2809	2425	2157
10	3371	3084	2793	2534
15	3465	3235	3010	2762
20	3201	3312	3135	2936
25	2824	3364	3226	3045

Table 4. Freeway throughput (veh/hr/ln) at the off-ramp area under various maximum CACC string length and inter-string time gap levels.

Max string length	Inter-string time gap (s)			
	1.0	1.5	2.0	2.5
5	3115	2822	2422	2157
10	3335	3078	2797	2536
15	3474	3265	3016	2770
20	3139	3317	3149	2934
25	2808	3367	3234	3046

Based on the above analyses, we recommend that the maximum string length should be in the range between 10 and 15; and the inter-string gap should be between 1.0 and 1.5 seconds. With those parameter levels, the traffic stream at the freeway on/off-ramp bottlenecks can reach a high-level throughput, while string stable operation can also be maintained. In the following capacity and throughput analyses, we have used the maximum string length of 10 and the inter-string time gap of 1.5 seconds. We adopted the conservative end of the recommended range because our analysis scenarios may have on-ramp and off-ramp traffic inputs larger than 500 veh/hr. Using these parameter values can lower the probability of traffic breakdown for those challenging cases.

PIPELINE CAPACITY OF MULTI-LANE FREEWAY

Pipeline Capacity by PATH and MOTUS

Table 5 shows the pipeline capacity estimated by the PATH and MOTUS models with a 20% increase of CACC market penetration rates. In the case of 0% CACC, the pipeline capacity of the human driver models by the models are both around 2120 veh/h/lane, indicating that these two calibrated human driver models are consistent in producing similar and comparable results. After adding CACC vehicles in the traffic, the pipeline capacity rises with the number of CACC vehicles by both the PATH and MOTUS models. In low MPRs, the capacity increases slowly at the 20% and 40% MPRs, however, the growth becomes sharp in high MPRs cases that reaching at least 20%, 40% and 60% of increment in the case of 60%, 80% and 100% CACC.

Table 5. Pipeline capacity (veh/h/lane) and its growth with market penetration rates by the PATH and MOTUS models.

	CACC Market Penetration Rates					
	0%	20%	40%	60%	80%	100%
PATH	2120	2209	2415	2723	3106	3465
Growth	0	4.20%	13.90%	28.40%	46.50%	63.40%
MOTUS	2124	2222	2353.2	2619.8	3091.8	3824.4
Growth	0	4.62%	10.79%	23.34%	45.56%	80.06%

High consistency is found in the results by the PATH model and MOTUS model, except for the case of 100% CACC vehicles. Possible explanations for the discrepancy might be:

- The vehicle generating algorithm. PATH ensures a steady state when the CACC vehicles are generated and placed in the network, while MOTUS has less strict rules in generating CACC vehicles. With this constraint, the PATH model generates fewer vehicles at the source link than the MOTUS model and therefore the maximum throughput that has been detected is smaller.
- The lane change model. The PATH model and MOTUS model are based on different lane change models, which lead to different lane change behavior. For discretionary lane changes in the pipeline simulations, moderate lane changes are expected in MOTUS without causing large disturbances to another lane, while the lane changes from the PATH simulations can be more aggressive and result in more disturbance.
- The vehicle length. Initially, the vehicle length is assumed different as 5 meters and 4 meters in the PATH and MOTUS models when the model calibrations were conducted separately. Later for comparable results, these values are inherited in the CACC simulations and that inevitably causes a significant difference in the pipeline capacity.

Pipeline Capacity with CACC operation strategies

Figure 6 shows the freeway mainline capacity as a function of the CACC market penetration, under various CACC operation strategies. The curve of the base case shows the results when no strategy was implemented. The ML strategy was applied only at 40%, 60% and 80% CACC market penetrations. At 40% penetration, the leftmost lane of the freeway was operated as the managed lane; whereas at 60% penetration the two leftmost lanes and at 80% penetration the three leftmost lanes. The VAD was used between 20% and 80% CACC market penetrations. It was assumed that all manually driven vehicles were equipped with the VAD. The DLC restriction strategy was implemented for all CACC market penetrations.
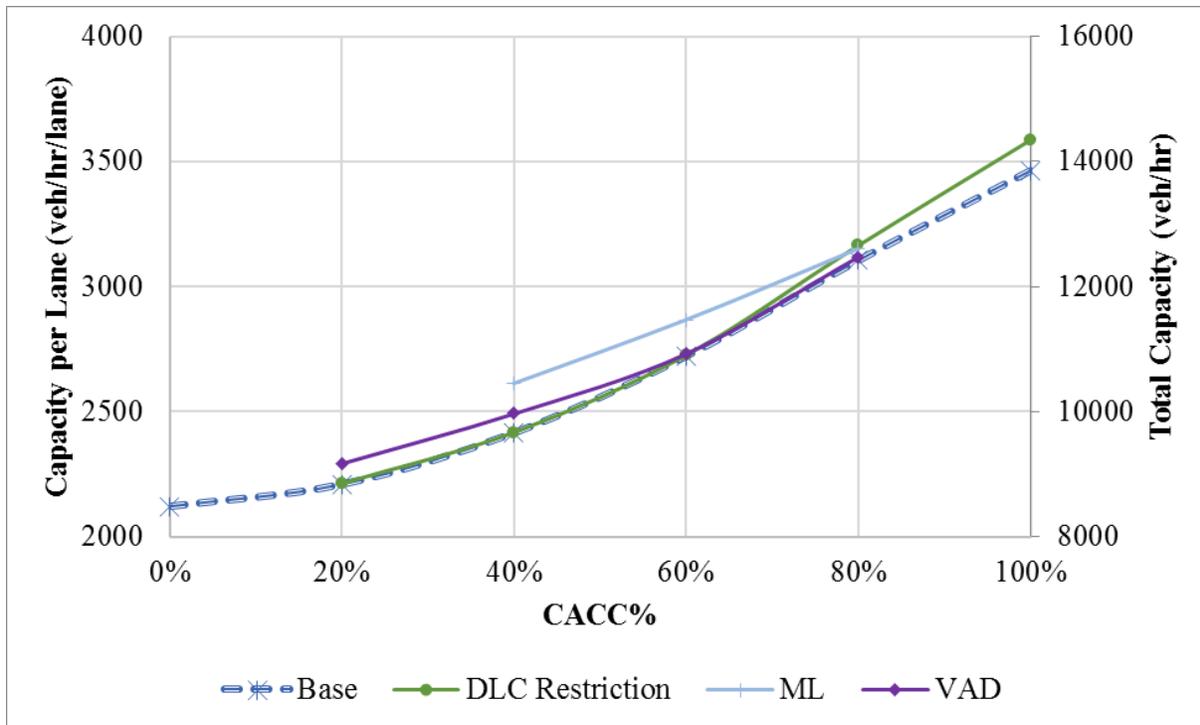
Figure 8. Graph. Freeway capacity at different CACC market penetrations. The horizontal axis of this graph depicts CACC market penetration and ranges from 0 percent to 100 percent. The vertical axis represents capacity of the simple network (vehicles per hour). The left vertical axis represents the per lane capacity and ranges from 2000 to 4000. The right vertical axis represents the total capacity of the 4 lanes and ranges from 8000 to 16000. The graph shows four lines starting at 0 percent on the horizontal axis and 2120 on the left vertical axis. The blue dashed line (representing base case where no CACC operation strategies are deployed) starts at 0 percent on the horizontal axis and 2120 on the vertical axis and then climbs quadratically and ends at 100 percent on the horizontal axis and 3465 on the vertical axis. The green solid line (representing DLC restriction case) falls along the same trajectory, but ends at 100 percent on the horizontal axis and 3585 on the vertical axis. The blue solid line (representing ML case) starts at 40 percent on the horizontal axis and 2415 on the vertical axis, curving through 60 percent on the horizontal axis and 2612 on the vertical axis, peaking the graph at 80 on the horizontal axis and 3151 on the vertical axis. The purple solid line (representing VAD case) starts at 20 percent on the horizontal axis and 2293 on the vertical axis, curving through 40 percent on the horizontal axis and 2492 on the vertical axis, peaking and leaving the graph at 80 on the horizontal axis and 3119 on the vertical axis.

The curve for the base case has a quadratic trend, which indicates that the capacity increases more rapidly once the market penetration of CACC equipped vehicles becomes larger. At 100% market penetration, the freeway capacity is roughly 63% higher than at 0% market penetration. The results also indicate that the ML strategy can bring about more capacity improvement at 40% and 60% penetrations than at 80% penetration. For the VAD strategy, the most significant benefit is observed at lower penetration cases (e.g., 20% and 40%); whereas the DLC restriction strategy works better at high penetration cases (e.g., 80% and 100%).

The ML strategy has two major effects on the traffic flow. It increases the number of CACC vehicle strings in the managed lane and subsequently improves the capacity of the lane. On the other hand, this strategy reduces the CACC penetration in the general-purpose lanes and thus makes their capacity lower. At 40% and 60% CACC market penetrations, the capacity increase of the managed lanes is substantially larger than the capacity decrease of the general-purpose lanes, leading to an overall improvement of the freeway capacity. At 80% penetration, however, the capacity of each lane is already at a high level without the ML strategy. After the managed lanes are implemented, the capacity reduction of the general-purpose lane is so great that it offsets the capacity increase of all three managed lanes.

Because the VAD strategy helps the CACC vehicles find a CACC vehicle string leader, it increases the probability that a CACC vehicle operates in a CACC string. The probability that a CACC vehicle is in a CACC string is estimated by using the law of total probability (see table 5). Results in the table suggest that the VAD strategy brings about substantial improvement of the CACC string operation at low and medium CACC market penetrations. When the CACC market penetration grows to 80%, the benefit of this strategy is only marginal. The theoretical probability analysis explains the observation that the VAD strategy only creates a capacity improvement at medium and low CACC market penetration cases when the manually driven VAD vehicles are a larger fraction of the total vehicle population.

Table 6. Probability that a CACC vehicle operates in a CACC string.

	CACC Market Penetration			
	20%	**40%**	**60%**	**80%**
Without VAD	36%	64%	84%	96%
With VAD	100%	100%	100%	100%
Difference	64%	36%	16%	4%

The DLC restriction strategy has little impact when the CACC market penetration is 60% or lower. In these cases, the manually driven vehicles will make discretionary lane changes regardless of whether the strategy is implemented or not. As the manually driven vehicles make discretionary lane changes, they create disturbances to the traffic stream, and eventually affect the CACC string operation. At high CACC market penetrations, most drivers are affected by the strategy. In this case, it can significantly reduce the disturbances caused by vehicles' discretionary lane changes. In addition, the traffic density is much higher in the high CACC market penetration cases. Reducing the lane change disturbances can create greater improvement in the busy traffic flow than in the light traffic flow.

We can also compare the simulation results with the theoretical capacity. When the CACC market penetration is 100%, the theoretical capacity can be reached in an ideal car-following condition—without disturbances caused by the lane change maneuvers, no heterogeneous behaviors among drivers, and perfect CACC vehicle string operations. The theoretical capacity at 100% market penetration is 3721 veh/hr/lane based on Varaiya, (1993). As figure 6 shows, the simulated capacity is about 93% of the theoretical capacity for the base case, and 96% for the DLC restriction case. The simulated capacity is lower than the theoretical capacity for the following reasons:

- Discretionary lane changes cause lateral interactions and additional decelerations, thereby reducing the capacity.
- String leaders may have a lower than average desired speed because the desired speed of the driver population follows a distribution rather than being a single deterministic value. This can impede the flow of subsequent vehicles in the CACC string.
- The CACC string may not always operate at its maximum length. When the length is less than the maximum, the capacity improvement becomes less.

FREEWAY CAPACITY AT MERGE BOTTLENECKS

The previous pipeline capacity analysis suggests that the capacity improvement has a quadratic trend with the CACC market penetration. In the following analysis, we will check if such a trend still exists when there is merging traffic from the on-ramp. The on-ramp merging traffic often triggers congestion of the freeway mainline traffic. If the CACC string operation can improve the traffic flow in the merging area, it subsequently enhances the overall performance of the freeway network. The quantitative impacts on traffic congestions are firstly explored by the study based on the MOTUS, aiming to show how replacing manual driving vehicles by the CACC vehicles can mitigate current recurrent congestion at merging bottlenecks. Latter, the characteristics of mixed traffic flows with various CACC market penetration rates are presented and analyzed by the PATH experiment.

Impacts of CACC Market Penetration Rates on Merging Bottlenecks

An experiment based on the simplified network was conducted to show the changes of traffic congestion at merging bottlenecks with an increase of CACC penetration rates. The main control variable is the CACC MPR which increases from 0% to 100% by an increment of 20%. The other control variable is the on-ramp demand, which represents different levels of traffic disturbance from on-ramps and might trigger various levels of congestion. The mainline demand is fixed at 2000 veh/h/lane, which is close to the pipeline capacity of manually driven vehicles. In this case, traffic disturbances can easily trigger congestion at the bottleneck, which represent the current bottleneck situations that we might have in the existing facility. The changes of congestion show the straightforward improvements introduced by CACC vehicles.

The speed contours of the merging bottleneck with two control variables are presented in figure 7. First, the congestion becomes less severe with the increase of CACC market penetration. At each demand level from the on-ramp, the congestion with 0% CACC is the most severe case and the congestion becomes either postponed or less severe, which suggests that CACC vehicles can reduce the speed reduction by congestion and improve the traffic performance at the merging bottleneck. That can be explained by the fact that with more CACC vehicles, more CACC short gaps are applied, which leaves more spacing for the merging traffic. Thus, the merging traffic causes less disturbance to the mainline traffic. So even without cooperative merging maneuvers, the merging efficiency spontaneously increases with the number of CACC vehicles.

The positive impacts by CACC vehicles are compensated by the merging disturbance. At each MPR case in figure 7, large on-ramp demand deteriorates the congestion the same way as it does to the current traffic without CACC vehicles. At several low MPRs, the traffic performance with

CACC vehicles is not substantially better than the reference cases. This implies that a small number of CACC vehicles may not be able to show direct benefits in merging bottlenecks with large merging traffic flows. In the near future, low CACC MPR is beneficial to low-demand bottlenecks and the impacts of CACC vehicles should not be overestimated.
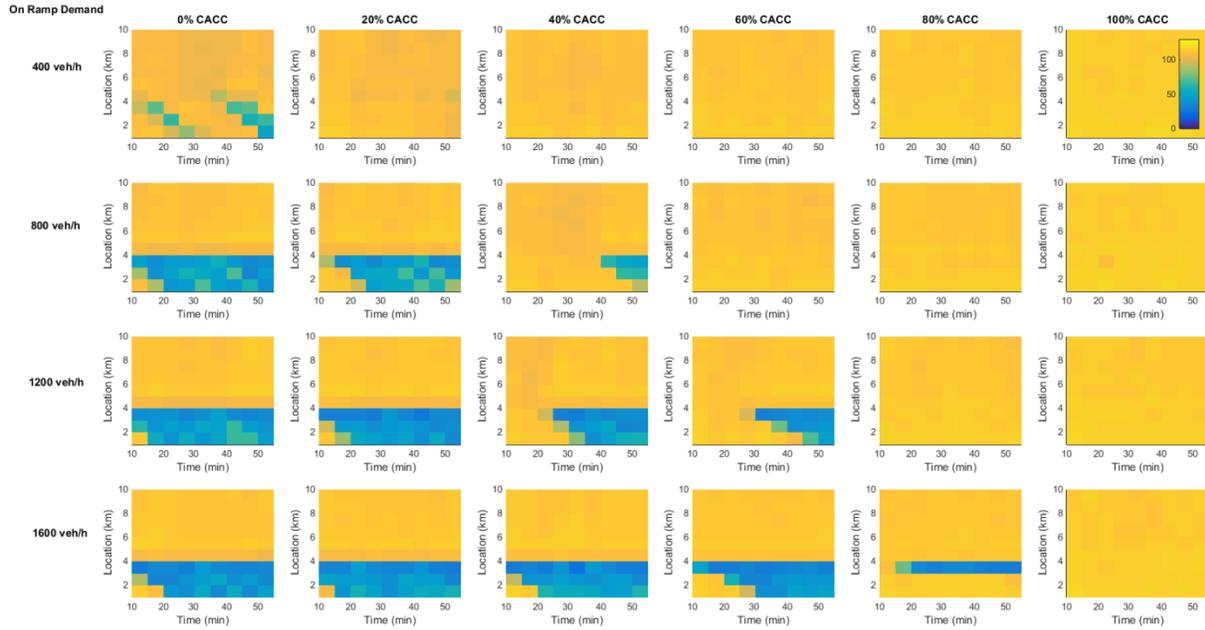
Figure 9. Graph. Traffic performance in speed contour with various CACC market penetration rates and on ramp demand. There are 24 speed contours placed in a 6 ×4 matrix, where the row and column represent the CACC market penetration rates and the on ramp demand respectively. In each row, the on ramp demand is fixed and the subfigures show the speed contour changes with CACC market penetration rates increasing from 0% to 100%. Each column represents the speed contour with fixed CACC market penetration rate, with on ramp demand increase from 400 veh/h at the top to 1600 veh/h at the bottom. With 400 veh/h on ramp demand, slight speed reductions can be observed in 0% CACC cases, while no congestion was founded at increased CACC% cases. With 800 veh/h on ramp demand, long-lasting congestion appears in 0% and 20% cases and the congestion was postponed for 40 mins with 40% CACC vehicles. In the scenario of 1200 veh/h on-ramp demand, severe congestion is observed at 0% and 20% and postponed congestion is shown at 40% and 60%. With the extreme on-ramp demand of 1600 veh/h, congestion appears in every low CACC% case until the 80% CACC cases that congestion became less severe and does not propagate upstream. In 100% CACC cases, no congestion appears in all simulation cases.

In a quantitative analysis, table 6 shows the decreased travel time delay with increased CACC market penetration rates. The previous pipeline capacity experiment suggests that CACC vehicles have the potential to increase the road capacity. Because of that, a trend is found that higher CACC MPRs experience less congestion and thus cause less travel time delay. The delay drop is often dramatic wherever the congestion is prevented. The 20% CACC vehicles with 1200 and 1600 veh/h/lane on-ramp demand are two exceptions found in Table 6. When CACC vehicles increase from 0% to 20%, there has been a slight rise in the delay for both cases. The results indicate that 20% CACC MPRs cannot cope with a high disturbance from the on ramp

and even shows negative impacts compare to the scenario with 100% manually driven vehicles. A possible explanation for this might be that the expected small improvement by CACC vehicles is compensated by the CACC system deactivations in the merging process. Due to the large on-ramp demand, cooperative lane changes are often requested and CACC vehicles have to be deactivated and switched to manual control. This deactivation inevitably leads to large gaps in the following manual-driven mode, which is related to small throughput and large delay.

Table 7. Averaged Travel Time Delays with CACC Market Penetration Rates.

On-ramp Demand	CACC %					
	0% CACC	20% CACC	40% CACC	60% CACC	80% CACC	100% CACC
400	89.1	54.7	43.0	38.2	32.3	27.9
800	240.8	187.6	126.8	40.4	33.9	28.5
1200	283.5	308.5	257.0	157.1	34.7	29.6
1600	294.0	317.8	300.7	248.9	124.0	30.2

Merging Capacity with CACC operation strategies

Results presented in the previous section also indicate that the ML and VAD strategy may relieve the congestion of a freeway merge bottleneck. The ML strategy attracts CACC vehicles to the managed lane and subsequently helps create extra gaps in the freeway general-purpose lane so that the on-ramp traffic can merge into the mainline more easily. The VAD strategy allows the on-ramp CACC vehicles to join a CACC string leader immediately after they enter the freeway mainline. It thus increases the queue discharging flow rate. The DLC strategy is expected to have little impact on traffic operations in the merging area because it only affects the discretionary lane change maneuvers, while the merging vehicles must make mandatory lane changes to enter the freeway. For the above reasons, we emphasize the impact analysis of the ML and VAD strategies in this section.

We first examined the freeway throughput when there was no CACC operation strategy (see figure 7). The figure shows that the throughput reduces as the on-ramp traffic increases. But the throughput still has the quadratic increase trend as the CACC market penetration grows. This finding confirms our expectation that the CACC string operation can improve the performance of the on-ramp merging area. The figure also suggests that the freeway throughput becomes substantially lower than the freeway capacity when the on-ramp traffic volume grows.
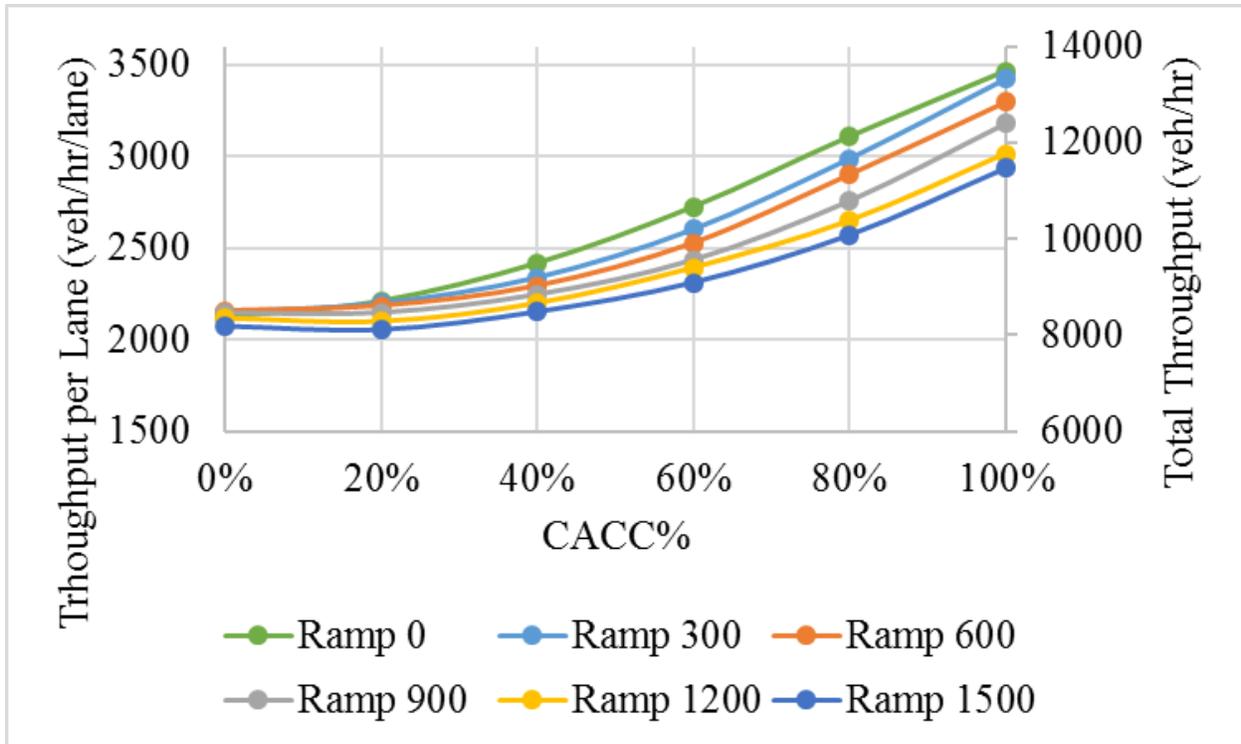
Figure 10. Graph. Throughput of the freeway merge bottleneck. The horizontal axis of this graph depicts CACC market penetration and ranges from 0 percent to 100 percent. The vertical axis represents throughput of the simple network (vehicles per hour). The left vertical axis represents the per lane throughput and ranges from 1500 to 3500. The right vertical axis represents the total throughput of the 4 lanes and ranges from 6000 to 14000. The graph shows six lines starting at 0 percent on the horizontal axis and 2074 on the left vertical axis. All lines represent a quadratic increase trend. The green solid line (representing 0 on-ramp input case) falls to 0 percent on the horizontal axis and 2120 on the vertical axis and then climbs quadratically and ends at 100 percent on the horizontal axis and 3465 on the vertical axis. The light blue solid line (representing 300 vehicles per hour on-ramp input case) falls to 0 percent on the horizontal axis and 2147 on the vertical axis and then climbs quadratically and ends at 100 percent on the horizontal axis and 3422 on the vertical axis. The red solid line (representing 600 vehicles per hour on-ramp input case) falls to 0 percent on the horizontal axis and 2156 on the vertical axis and then climbs quadratically and ends at 100 percent on the horizontal axis and 3294 on the vertical axis. The gray solid line (representing 900 vehicles per hour on-ramp input case) falls to 0 percent on the horizontal axis and 2145 on the vertical axis and then climbs quadratically and ends at 100 percent on the horizontal axis and 3178 on the vertical axis. The yellow solid line (representing 1200 vehicles per hour on-ramp input case) falls to 0 percent on the horizontal axis and 2117 on the vertical axis and then climbs quadratically and ends at 100 percent on the horizontal axis and 3014 on the vertical axis. The dark blue solid line (representing 1500 vehicles per hour on-ramp input case) falls to 0 percent on the horizontal axis and 2074 on the vertical axis and then climbs quadratically and ends at 100 percent on the horizontal axis and 2934 on the vertical axis.

After the ML and VAD strategies were implemented, the pattern of the traffic flow became different (see figure 8 for the 40% CACC case; other cases have similar trends). With these strategies, the freeway mainline can serve more on-ramp traffic without traffic breakdown. In this case, the freeway throughput increases as the on-ramp traffic volume grows from 300 veh/hr to 600 veh/hr. When the on-ramp traffic is 900 veh/hr or larger, the merging area becomes congested and the throughput starts decreasing. Nonetheless, the throughput with ML or VAD is still larger than the base case, indicating that those strategies can help improve the traffic flow dynamics even after the traffic becomes congested. figure 8 also suggests that the VAD strategy can create greater improvement in the throughput than the ML strategy. With the VAD strategy, the CACC vehicles from the on-ramp can easily join a string leader and then exit the merging area in a CACC string. In this case, the queue discharging flow becomes more efficient. With the ML strategy, there are more gaps in the rightmost lane, which allows the on-ramp traffic to merge more easily. But the vehicles remaining in the rightmost lane are mostly manually driven vehicles. In this case, the probability for the on-ramp CACC vehicles to form CACC strings in the merging area is smaller than in the base case. Consequently, the throughput of the rightmost lane becomes smaller under the ML strategy. Such a reduction of the throughput in the rightmost lane offsets the throughput improvement due to the enhanced CACC string operation in the managed lane.
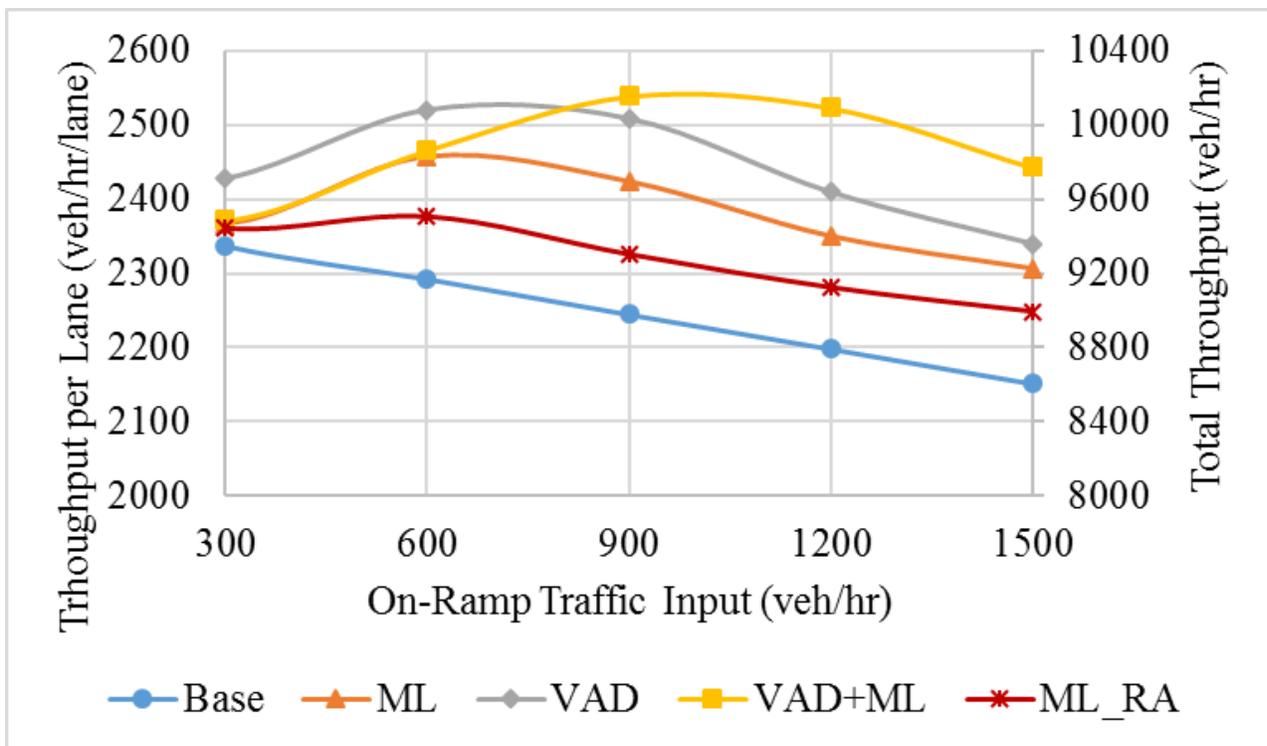
Figure 11. Graph. Throughput of the freeway merging bottleneck under various management strategies and 40% CACC market penetration. The horizontal axis of this graph depicts on-ramp traffic input (vehicles per hour) and ranges from 300 to 1500. The vertical axis represents throughput of the simple network (vehicles per hour). The left vertical axis represents the per lane throughput and ranges from 2000 to 2600. The right vertical axis represents the total throughput of the 4 lanes and ranges from 8000 to 10400. The graph shows

31

five lines starting at 0 percent on the horizontal axis and 2415 on the left vertical axis. The blue solid line (representing base case where no CACC operation strategies are implemented) falls to 300 on the horizontal axis and 2337 on the vertical axis and then decreases linearly and ends at 1500 on the horizontal axis and 2152 on the vertical axis. The orange solid line (representing ML case) falls to 300 on the horizontal axis and 2367 on the vertical axis and then increases to 600 on the horizontal axis and 2456 on the vertical axis, and then starts to decrease and ends at 1500 on the horizontal axis and 2306 on the vertical axis. The gray solid line (representing the VAD case) falls to 300 on the horizontal axis and 2428 on the vertical axis and then increases to 600 on the horizontal axis and 2520 on the vertical axis, and then starts to decrease and ends at 1500 on the horizontal axis and 2340 on the vertical axis. The yellow solid line (representing ML and VAD combined case) falls to 300 on the horizontal axis and 2371 on the vertical axis and then increases to 900 on the horizontal axis and 2538 on the vertical axis, and then starts to decrease and ends at 1500 on the horizontal axis and 2443 on the vertical axis. The red solid line (representing ML with restricted access case) falls to 300 on the horizontal axis and 2360 on the vertical axis and then increases to 600 on the horizontal axis and 2376 on the vertical axis, and then starts to decrease and ends at 1500 on the horizontal axis and 2248 on the vertical axis.

In the previous analysis, we assumed continuous access for the managed lane. The ML strategy can also apply with restricted access (RA) such that the CACC vehicles may only enter and exit the managed lane at designated ingresses and egresses. To test the traffic flow performance under the restricted access operation, we have added a managed lane entry segment in the simulation network. Based on FHWA's guidance (Neudorff et al., 2003), the entry segment is 600 meters downstream from the end of the on-ramp acceleration lane and the length of the entry is 400 meters. When the restricted access was implemented in simulation (ML_RA curves in figure 8), CACC vehicles could not make lane changes from the general-purpose lane to the managed lane upstream of the merging area. In this case, they were unable to create gaps for the on-ramp merging vehicles. When they arrived at the entry point downstream from the merging area, the traffic flow was already in a free flow condition. There was no longer any incentive for them to make lane changes towards the managed lane, so the managed lane was underused.

Since both the ML and VAD strategy can improve throughput, the performance of the merging area might be further increased if the two strategies are applied at the same time. The results for the combined strategy case are also shown in figure 8. Interestingly, the combined strategy only brings about significant benefit when the on-ramp traffic input is 900 veh/hr or higher. Under lower on-ramp inputs, the effect of the combined strategy is almost identical to that of the ML strategy alone. It suggests that the VAD strategy does not create extra improvement at low on-ramp input conditions once the ML strategy is activated. When the ML is implemented, the CACC vehicles are concentrated in the managed lane and most vehicles in the general-purpose lanes are manually driven vehicles. In this case, the VAD strategy won't make much difference because there are not many CACC vehicles left. When the on-ramp traffic volume is small, only a few CACC vehicles will enter the freeway. These CACC vehicles are not enough to greatly change the fraction of CACC vehicles in the fleet. As the on-ramp traffic input reaches a high level (e.g., more than 900 veh/hr), the merging CACC vehicles start to significantly shift the fleet composition. The effect of the VAD strategy then becomes more prominent.

FREEWAY CAPACITY AT OFF-RAMP BOTTLENECKS

In this section, we identify the maximum off-ramp traffic volume the freeway off-ramp can serve while the freeway mainline remains in uncongested flow. The analysis was performed under various CACC market penetrations and with or without the CACC operation strategies discussed in the previous section. In the simulation runs, the freeway mainline input equaled the pipeline capacity measured at the respective CACC market penetrations. Then different percentages of the mainline traffic were assumed to exit the freeway through the off-ramp of the study network. The percentage of the mainline flow was used instead of the absolute traffic volume because we expected that the off-ramp traffic should be proportional to the mainline flow. The maximum percentage of the mainline traffic flow that can exit the freeway without disrupting the mainline flow is called the maximum off-ramp traffic percentage in the remainder of this section.
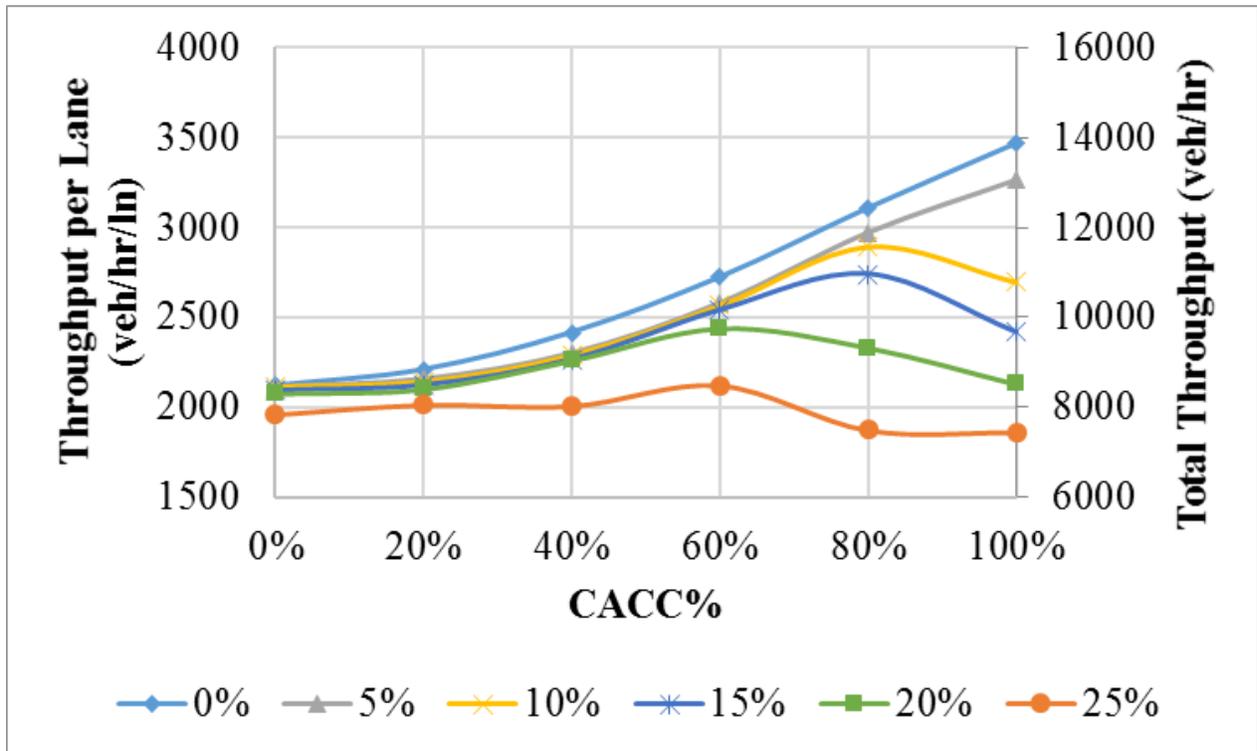
Figure 12. Graph. Freeway throughput of various off-ramp traffic percentages under the base case. The horizontal axis of this graph depicts CACC market penetration and ranges from 0 percent to 100 percent. The vertical axis represents capacity of the simple network (vehicles per hour). The left vertical axis represents the per lane capacity and ranges from 1500 to 4000. The right vertical axis represents the total capacity of the 4 lanes and ranges from 6000 to 16000. The graph shows six lines starting at 0 percent on the horizontal axis and 2120 on the left vertical axis. The blue solid line with diamond markers (representing 0 off-ramp traffic percentage) falls to 0 percent on the horizontal axis and 2120 on the vertical axis and then climbs quadratically and ends at 100 percent on the horizontal axis and 3465 on the vertical axis. The grey solid line (representing 5% off-ramp traffic) falls to 0 percent on the horizontal axis and 2114 on the vertical axis and then climbs quadratically and ends at 100 percent on the horizontal axis and 3263 on the vertical axis. The yellow solid line (representing 10 off-ramp traffic percentage) falls

to 0 percent on the horizontal axis and 2116 on the vertical axis and then increases to 80 percent on the horizontal axis and 2894 on the vertical axis, and then starts to decrease and ends at 100 percent on the horizontal axis and 2696 on the vertical axis. The blue solid line with star markers (representing 15 off-ramp traffic percentage) falls to 0 percent on the horizontal axis and 2096 on the vertical axis and then increases to 80 percent on the horizontal axis and 2741 on the vertical axis, and then starts to decrease and ends at 100 percent on the horizontal axis and 2419 on the vertical axis. The green solid line (representing 20 off-ramp traffic percentage) falls to 0 percent on the horizontal axis and 2079 on the vertical axis and then increases to 60 percent on the horizontal axis and 2435 on the vertical axis, and then starts to decrease and ends at 100 percent on the horizontal axis and 2131 on the vertical axis. The orange solid line (representing 25 off-ramp traffic percentage) falls to 0 percent on the horizontal axis and 1962 on the vertical axis and then increases to 60 percent on the horizontal axis and 2122 on the vertical axis, and then starts to decrease and ends at 100 percent on the horizontal axis and 1864 on the vertical axis.

Figure 9 shows the freeway throughput when no strategies are deployed. When the CACC market penetration is 60% or lower, up to 20% of the mainline traffic can exit the freeway without causing traffic breakdown. But when the CACC market penetration further increases, the maximum off-ramp traffic percentage decreases significantly. When the CACC penetration is 80%, the maximum off-ramp traffic percentage is between 15% and 20% and for the 100% CACC case it is only between 5% and 10%. The freeway can serve lower off-ramp traffic at higher CACC market penetration cases because the traffic density becomes very large in those cases. It is difficult for vehicles to find acceptable gaps to make discretionary or active lane changes towards the off-ramp lane. As the exiting vehicle is close to the off-ramp but still cannot merge into the off-ramp, the driver must make aggressive mandatory lane changes, which cause strong disturbances to the traffic stream. Such disturbances can easily propagate upstream and develop into heavy shockwaves in the dense traffic flow. In addition, most the exiting vehicles are CACC vehicles in the high CACC market penetration cases. When a CACC vehicle wants to exit, the driver needs to first turn off the CACC and manually make the lane change. Such a behavior will break the CACC string operation and further reduce the throughput.

The ML strategy can decrease the performance of the off-ramp bottleneck. As the strategy is implemented, the leftmost lane takes more traffic. When those vehicles need to exit the freeway, they make extra lane changing maneuvers, which can cause extra disturbances to the traffic flow. With this strategy, the maximum off-ramp traffic percentage reduces to a level between 5% and 10% under 80% CACC penetration. Under 60% CACC penetration, the maximum off-ramp traffic percentage reduces to a level between 10% and 15%. When the CACC market penetration is 40%, the ML strategy does not significantly reduce the throughput of the off-ramp area. The VAD strategy can slightly improve the throughput when the off-ramp traffic does not exceed the maximum off-ramp traffic percentage. Once the off-ramp traffic becomes larger than the maximum percentage, the throughput is smaller under the 60% and 80% CACC market penetration cases. The level of the maximum off-ramp traffic percentage is the same with and without the VAD strategy.

The above analysis shows that the freeway off-ramp areas may become major bottlenecks as the off-ramp volume increases due to the increase of the freeway throughput with the CACC market penetration. The traffic management strategies that increase the capacity and throughput for the basic freeway segments and merge areas may reduce the performance of the off-ramp area. To

improve the operation, we can recommend drivers to start making lane changes towards the freeway exit earlier than they normally do. In this case, most them can make discretionary or active lane changes instead of aggressive mandatory lane changes before the exit. As the number of mandatory lane changes reduces, the severe disturbances in the traffic stream also decrease. In addition, we can keep the CACC vehicles in the CACC mode if the driver cannot find an acceptable gap in the target lane when he is trying to perform discretionary or active lane changes towards the exit. In this case, we reduce the number of mode switches for the CACC drivers and thereby lower the probability that the CACC string operation is interrupted.

The above improvement strategy has been implemented in the simulation. Before the improvement, the exiting drivers would start searching gaps in the right lane 1.5 kilometers upstream from the off-ramp. With the improvement, the drivers start the lane change process 3 kilometers upstream. The traffic improves significantly due to this strategy. At 100% CACC penetration, the maximum off-ramp traffic percentage increases to a level between 15% and 20%. The throughput reduction after the off-ramp traffic exceeds the maximum percentage also becomes much smaller.

IMPACT OF ACC OPERATION ON TRAFFIC FLOW

In addition to the impact analysis for the CACC vehicle operation, we have examined the capacity and throughput for the simple network under various ACC market penetrations. We applied the same simulation experiment setup for the ACC study as we performed the CACC studies. The simulation network is the simple network shown in Figure 1. In addition to the pipeline capacity analysis, we also investigated the freeway throughput for the on-ramp bottleneck and the off-ramp bottleneck.

The pipeline capacity and freeway throughput under various ACC market penetrations are depicted in figure 10. Because the ACC operation decreases the stability of the traffic flow, we observe a decrease trend of the pipeline capacity as the ACC market penetration increases. We also observe a linear decrease trend of the throughput with the ACC market penetration, regardless of the on-ramp input. Especially when the ACC market penetration is 100%, the throughput will have a significant decrease although the on-ramp input is very small. It indicates that the traffic stream under 100% ACC is unstable. A minor disturbance from the on-ramp can cause traffic flow breakdown, and subsequently lead to a queue discharging flow reduced to 1800 vehicles per hour per lane.

The ACC operation can negatively impact the operation of the off-ramp bottleneck as well. As the ACC market penetration increases, the freeway throughput at the off-ramp area also reduces linearly, regardless of the percentage of the off-ramp traffic (see figure 11). The analysis results indicate that the implementation of ACC cannot improve the overall performance of the freeway.
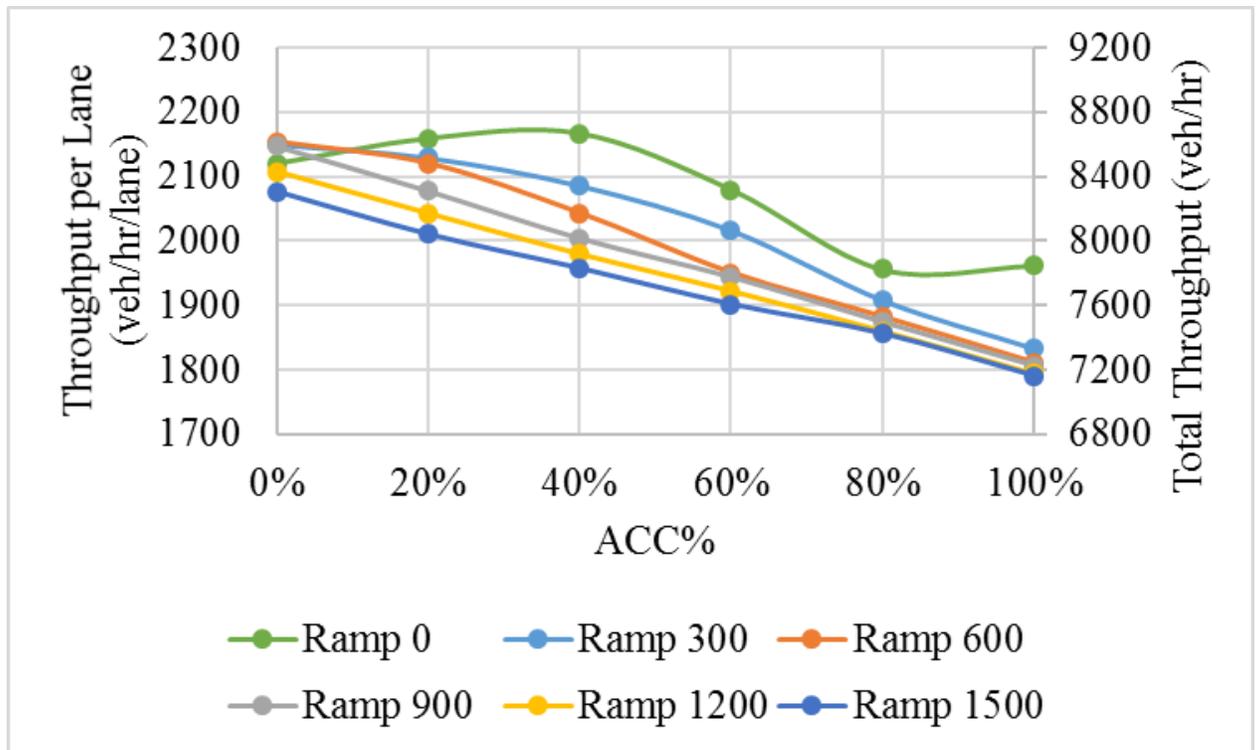
Figure 13. Graph. Freeway throughput with ACC at multiple market penetrations with various on-ramp traffic inputs (veh/hr/ln). The horizontal axis of this graph depicts ACC market penetration and ranges from 0 percent to 100 percent. The vertical axis represents throughput of the simple network (vehicles per hour). The left vertical axis represents the per lane throughput and ranges from 1700 to 2300. The right vertical axis represents the total throughput of the 4 lanes and ranges from 6800 to 9200. The graph shows six lines starting at 0 percent on the horizontal axis and 2153 on the left vertical axis. All lines represent a decreasing increase trend. The green solid line (representing 0 on-ramp input case) falls to 0 percent on the horizontal axis and 2120 on the vertical axis and then reduces and ends at 100 percent on the horizontal axis and 1962 on the vertical axis. The light blue solid line (representing 300 vehicles per hour on-ramp input case) falls to 0 percent on the horizontal axis and 2150 on the vertical axis and then reduces linearly and ends at 100 percent on the horizontal axis and 1834 on the vertical axis. The red solid line (representing 600 vehicles per hour on-ramp input case) falls to 0 percent on the horizontal axis and 2153 on the vertical axis and then reduces linearly and ends at 100 percent on the horizontal axis and 1811 on the vertical axis. The gray solid line (representing 900 vehicles per hour on-ramp input case) falls to 0 percent on the horizontal axis and 2148 on the vertical axis and then reduces linearly and ends at 100 percent on the horizontal axis and 1806 on the vertical axis. The yellow solid line (representing 1200 vehicles per hour on-ramp input case) falls to 0 percent on the horizontal axis and 2107 on the vertical axis and then reduces linearly and ends at 100 percent on the horizontal axis and 1794 on the vertical axis. The dark blue solid line (representing 1500 vehicles per hour on-ramp input case) falls to 0 percent on the horizontal axis and 2077 on the vertical axis and then reduces linearly and ends at 100 percent on the horizontal axis and 1791 on the vertical axis.
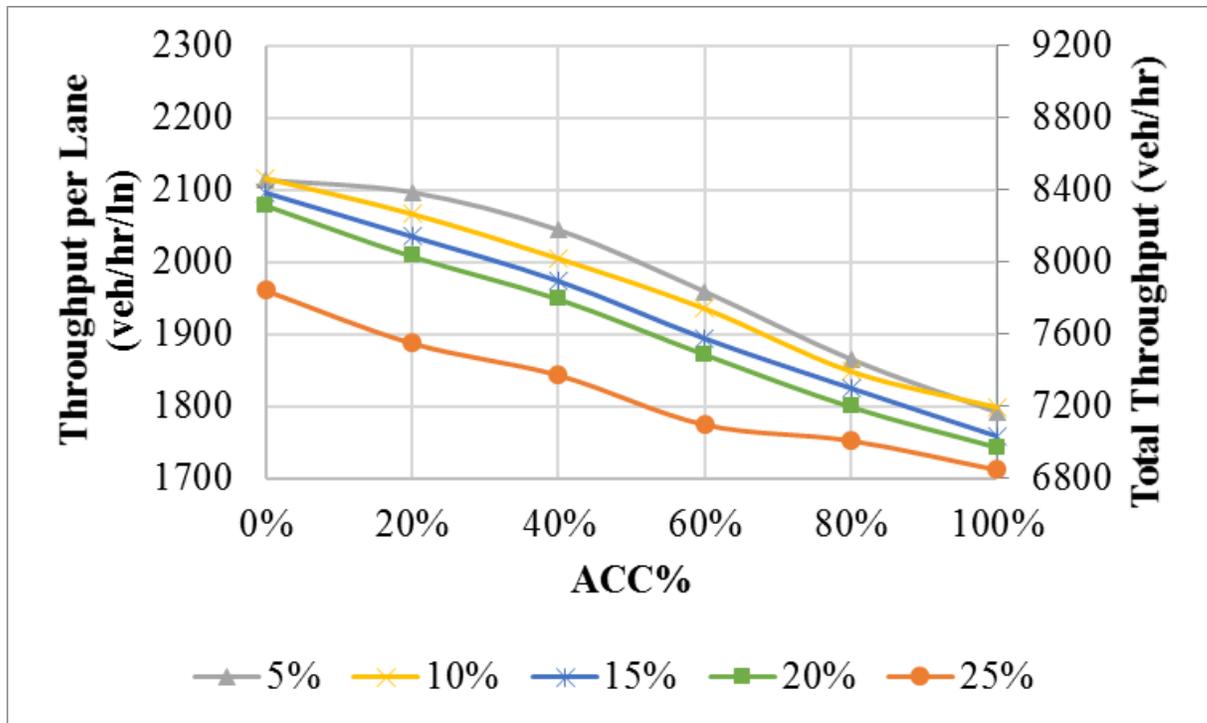
Figure 14. Graph. Freeway throughput with ACC at different market penetrations and various off-ramp traffic percentages. The horizontal axis of this graph depicts ACC market penetration and ranges from 0 percent to 100 percent. The vertical axis represents throughput of the simple network (vehicles per hour). The left vertical axis represents the per lane capacity and ranges from 1700 to 2300. The right vertical axis represents the total capacity of the 4 lanes and ranges from 6800 to 9200. The graph shows five lines starting at 0 percent on the horizontal axis and 2116 on the left vertical axis. The grey solid line (representing 5% off-ramp traffic) falls to 0 percent on the horizontal axis and 2114 on the vertical axis and then decreases linearly and ends at 100 percent on the horizontal axis and 1792 on the vertical axis. The yellow solid line (representing 10 off-ramp traffic percentage) falls to 0 percent on the horizontal axis and 2116 on the vertical axis and then decreases linearly and ends at 100 percent on the horizontal axis and 1798 on the vertical axis. The blue solid line with star markers (representing 15 off-ramp traffic percentage) falls to 0 percent on the horizontal axis and 2096 on the vertical axis and then decreases linearly and ends at 100 percent on the horizontal axis and 1757 on the vertical axis. The green solid line (representing 20 off-ramp traffic percentage) falls to 0 percent on the horizontal axis and 2079 on the vertical axis and then decreases linearly and ends at 100 percent on the horizontal axis and 1743 on the vertical axis. The orange solid line (representing 25 off-ramp traffic percentage) falls to 0 percent on the horizontal axis and 1962 on the vertical axis and then decreases linearly and ends at 100 percent on the horizontal axis and 1712 on the vertical axis.

RECOMMENDED CACC OPERATIONAL ALTERNATIVES FOR CORRIDOR IMPLEMENTATION

Based on the results of the studies of the operational alternatives on the simplified network discussed in the preceding sections, we developed the following recommendations regarding the

CACC operation strategies for the larger SR-99 network:

- The VAD strategy can improve the traffic operation for the basic freeway segments, on-ramp merging areas, and off-ramp diverging areas. It increases the probability that a CACC vehicle operates in a CACC string and reduces the probability that a CACC driver turns off the CACC mode. For these reasons, this strategy is recommended for implementation in the larger network.

- The ML strategy can be applied when the CACC market penetration is between 40% and 80%. It can improve the capacity and throughput for the basic freeway segments and on-ramp areas, although its influence becomes smaller as the CACC market penetration increases. However, it can negatively impact the performance of the off-ramp area when the CACC market penetration is 60% or larger. Therefore, we will use the ML strategy only under the 40% CACC market penetration or less in the SR-99 network.

- Since we will use the current traffic demand as the input for the SR-99 analysis, the off-ramp traffic should not cause heavy traffic congestion, regardless of the increase of the CACC market penetration. In this case, the traffic management for the off-ramp bottleneck will not be used.

MOBILITY PERFORMANCE OF CACC IN SR-99 NETWORK

Figure 12 shows the total VMT and VTT of the corridor. Since the demand input is the same for all the scenarios and the origin and destination for each vehicle is determined based on the observed OD matrix, the route of the simulated vehicles in each scenario is also identical. In this case, the total VMT has little change with the CACC market penetration. The total VTT decreases significantly as the CACC market penetration increases. It indicates that the traffic flow becomes less congested when there are more CACC vehicles in the traffic stream. We can also observe a rapid decrease of VTT when the CACC market penetration increases from 20% to 40%. In comparison, the total VTT is almost the same between 0% and 20% CACC market penetrations. It suggests that the CACC vehicle string operation cannot change the traffic flow pattern until the CACC market penetration reaches a level between 20% and 40%. The space mean speed has the same trend as the total VTT. As the CACC market penetration increases, the speed of traffic along the corridor also increases significantly.
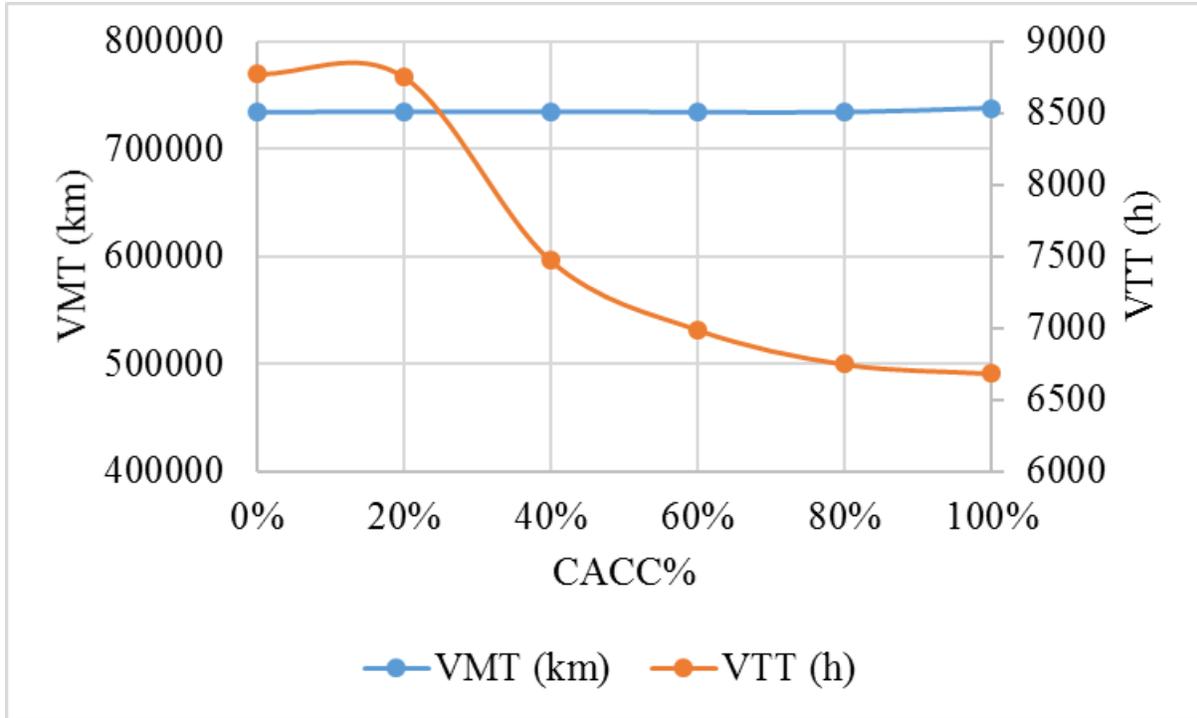
Figure 15. Graph. Total VMT and VTT. The horizontal axis of this graph depicts CACC market penetration and ranges from 0 percent to 100 percent. The left vertical axis represents the total vehicle miles traveled (kilometers) and ranges from 400000 to 800000. The right vertical axis represents the total vehicle time traveled (hours) and ranges from 6000 to 9000. The graph shows two lines. The blue solid line (representing VMT) falls to 0 percent on the horizontal axis and 734724 on the vertical axis and then stays almost flat and ends at 100 percent on the horizontal axis and 737895 on the vertical axis. The orange solid line (representing VTT) falls to 0 percent on the horizontal axis and 8773 on the vertical axis and then starts to decrease at 20 percent on the horizontal axis and 8754 on the vertical axis and ends at 100 percent on the horizontal axis and 6683 on the vertical axis.

The space mean speed contour plot (figure 13) suggests the same trend as the VTT plot: the traffic flow is greatly improved when the CACC market penetration is 40% or higher. Since there is little improvement at the 20% CACC case, we will examine if we can increase the mobility performance at this lower market penetration level via the CACC operation strategies.
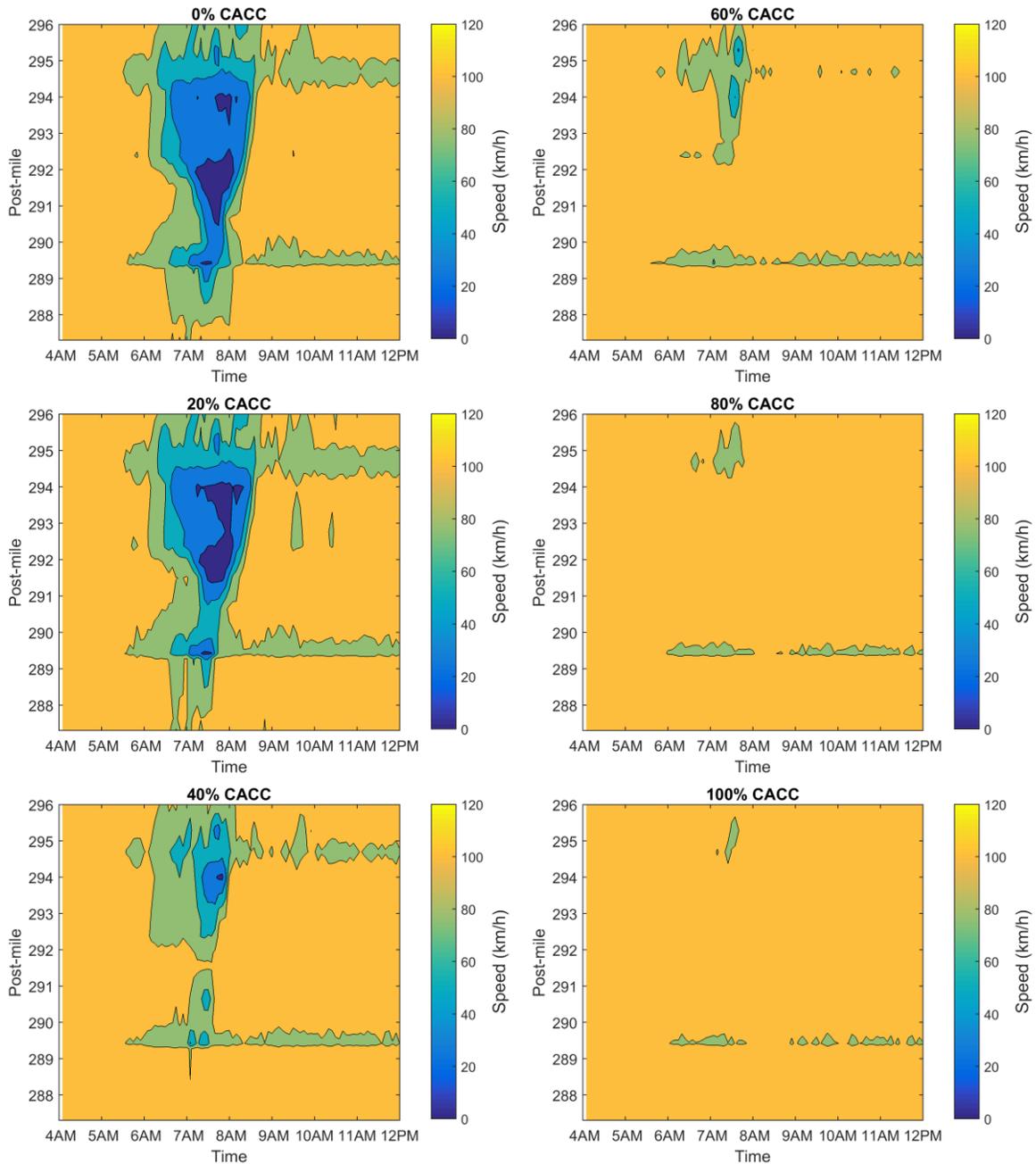
Figure 16. Illustration. Speed contour plot for each CACC market penetration. This figure shows the speed contour plot of the SR-99 corridor under various CACC market penetrations. The first plot of the left column shows the case of 0 percent CACC. It clearly shows the traffic congestion between 6:30 to 9:00 AM over the corridor. The second plot of the left column shows the case of 20 percent CACC. It has a similar pattern to the first plot. The third plot of the left column shows the case of 40 percent CACC. The traffic congestion is greatly relieved in this case. The three plots of the right column show the cases of 60, 80, and 100 percent CACC, respectively. The traffic congestion in those cases almost disappears.

40

The ML and VAD strategies were implemented for the 20% CACC market penetration case. The results show that the total VMT between the two cases is not substantially different (i.e., 0.08% difference). But the VMT time series have distinct patterns. Without the CACC operation strategy, the traffic was congested during the peak hours (e.g., from 6:00 to 8:30 am) and many vehicles waited in queues during that period. The queued vehicles contributed a great amount of VMT as the traffic congestion dissipated between 8:30 to 9:00 am. With the strategies, the traffic was not heavily congested and more vehicles could travel through the corridor during the peak hours, leading to a higher VMT between 6:00 to 8:30 am. Since there were not many queued vehicles, the VMT between 8:30 to 9:00 am was smaller than in the previous case. The operation strategies can decrease the total vehicle time traveled and increase the space mean speed for the peak hours. The mobility improvement due to the operation strategies can be depicted by the speed contour plots (figure 14). We can easily identify that the strategies can help both decrease the duration and the intensity of the traffic congestion at individual bottlenecks of the corridor.
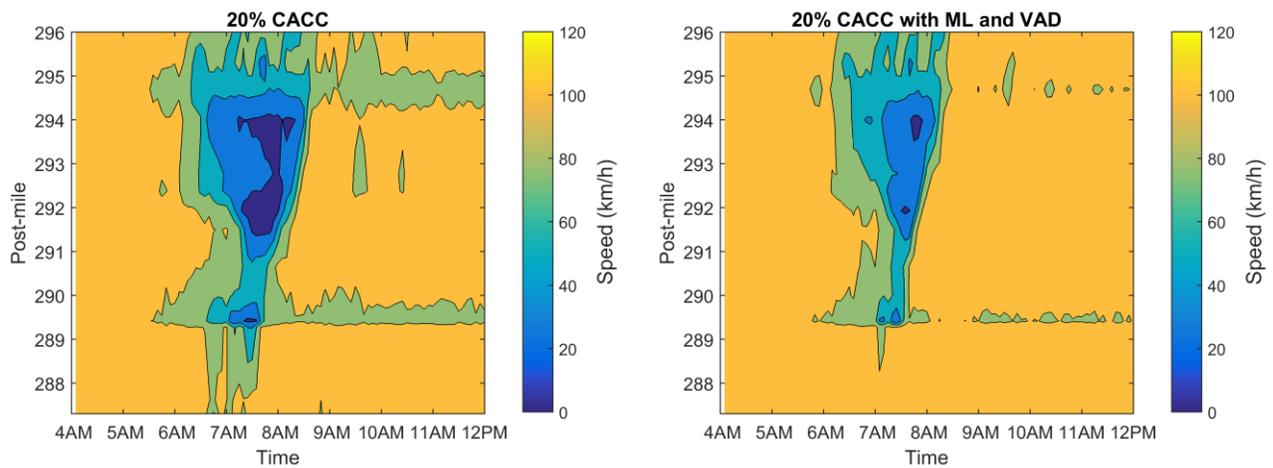
Figure 17. Illustration. Speed contour plot for 20% CACC market penetration with and without operation strategies. This figure shows the comparison of the speed contour plot before and after implementing the CACC operation strategies for the 20 percent CACC case. The left plot shows the results without the CACC operation strategies. The traffic is heavily congested between 6:30 and 9:00 AM. The right plot shows the results with the CACC operation strategies. The duration and intensity of traffic congestion is greatly reduced.

CHAPTER 6. CONCLUSIONS

SUMMARY OF STUDY FINDINGS

In this research, we have explored the impact of CACC vehicle string operations on freeway mobility performance. Particularly, we have examined the influence of CACC operation strategies in terms of improving the probability of forming and maintaining CACC vehicle strings in the traffic stream, and subsequently increasing the freeway capacity and throughput. For the homogeneous freeway segment, our analysis results indicate a quadratic increase trend of the pipeline capacity with the CACC market penetration. The pipeline capacity results were presented consistently by the PATH and MOTUS models, suggesting that the results of macroscopic impacts on capacity are concrete and reliable. Even though different CACC vehicle assumptions have been made and different human driver models were used in the PATH and MOTUS models, the resulting pipeline capacity in each CACC market penetration rates are not significantly different from each other. The consistency implies that the simulation results are independent of traffic simulators without bias and hiding constraints, and both models are able to reproduce the CACC traffic streams that close to the reality. The ML and VAD strategy are most helpful under the low and medium CACC market penetrations (e.g., 20% to 60%) as they increase the probability for a CACC vehicle to operate in a CACC string. In addition, the ML strategy can greatly increase the average CACC string length in the managed lane. Under the high CACC market penetrations (e.g., 80% to 100%), the CACC strings are frequently interrupted by the discretionary lane change behaviors of vehicles within the string. In this case, the DLC restriction strategy has the most significant influence.

In the freeway on-ramp merging area, the throughput also increases quadratically with the CACC market penetration, although the improvement decreases substantially as the on-ramp traffic increases. The ML and VAD strategy can greatly change the traffic patterns of the merging area, and thus improve the traffic flow at the merge bottleneck. The ML strategy makes CACC vehicles concentrate in the managed lane, leading to a high output flow of the lane even when the on-ramp traffic volume is high. As the CACC vehicles move to the managed lane, the traffic flow in the rightmost lane becomes lighter. The on-ramp vehicles can find gaps in the rightmost lane more easily. With the VAD strategy, the on-ramp CACC vehicles can find a string leader as soon as they merge into the freeway mainline. Those vehicles can dispatch from the merging area more quickly when operating in the CACC string. After implementing the ML and VAD strategy at the same time, the throughput can be further increased, especially under high on-ramp input cases.

With the MOTUS model, different scenarios with the merging bottleneck were considered. In those cases, the mainline traffic input was set at the current mainline demand level. After replacing manually driven vehicles by CACC vehicles, the congestions are either mitigated or postponed, where nearly 10-50% of the travel time delay can be reduced. However, a negative impact of only replacing 20% CACC vehicles is found. As the on-ramp demand exceeds 1200 veh/h/lane, the congestion with 20% CACC vehicles is not substantially improved and the travel time delays increase up to 8%. The frequent CACC deactivations for cooperative lane changes at merging bottlenecks might be one explanation to that.

The traffic flow of the off-ramp area is expected to become worse if the off-ramp traffic flow increases proportionally with the mainline traffic as the CACC market penetration grows. The ML strategy might further degrade the throughput of the off-ramp area because of the disturbances caused by vehicles in the managed lane as they make lane changes towards the off-ramp. To improve the mobility performance of the off-ramp area, we have tested a strategy that offers early lane change advisory messages to the exiting vehicles. With the strategy, drivers will start making lane changes towards the exit at a further distance than they normally do. In this case, the aggressive lane changes performed by the exiting drivers near the end of the off-ramp can be greatly reduced. The analysis results show that this strategy can eliminate the off-ramp bottleneck when the off-ramp traffic is 20% of the mainline traffic or lower.

The traffic conditions for the SR-99 network improve significantly with the CACC market penetration. We have identified a critical CACC market penetration between 20% and 40%. Before the critical market penetration, the traffic flow dynamics is almost the same, regardless of the percentage of CACC vehicles in the traffic flow. When the CACC market penetration is higher than the critical level, the mobility performance improves rapidly. The critical CACC market penetration level can be further lowered by implementing the CACC operation strategies. After the ML and VAD strategy were implemented for the 20% CACC market penetration case, the VTT and space mean speed had a significant improvement. It suggests that we can achieve a high freeway mobility with proper CACC operation strategies when there are only a limited fraction of vehicles equipped with the CACC.

RECOMMENDATIONS FOR NEXT PHASE RESEARCH

To make accurate predictions of CACC impacts, we need a traffic simulation platform that can capture human drivers' behaviors, CACC drivers' behaviors, and the interactions of the two driver groups. Although we have developed such a platform in this study, there is still room to improve the modeling approach. For example, we use the same function to generate the lane change motivations for both the manual drivers and CACC drivers. Their gap search behaviors are also identical once they are in the before lane changing car following mode. It is likely that CACC drivers will have a different lane changing behavior pattern when they drive in the CACC mode. Such behavior patterns will require new models. In the absence of empirical data to support modeling how drivers actually behave, we can explore different behavioral assumptions to identify the behaviors that lead to the largest traffic improvements. Behaviors suggested by these models can be used as guidelines for developing future CACC control and cooperation algorithms.

We also recommend more CACC field tests in the future studies. Our current test datasets cover the CACC operation with mild disturbances under free flow conditions, and only for a single design of ACC and CACC systems. It is necessary to obtain data for other traffic conditions, especially congested conditions with shockwaves, and for a wider range of vehicle-following behaviors by ACC and CACC systems. The CACC vehicles' mode switch dynamics under various traffic conditions are also interesting to study. Moreover, the CACC drivers' lane changing behaviors and the manual drivers' lane changing behaviors ahead of or behind CACC vehicle strings are important traffic conditions to observe in the field. Those datasets can help us

develop more accurate human driver and CACC vehicle behavior models, which will generate better predictions regarding the congestion improvements due to CACC operations.

The current research has considered the CACC operation strategies that do not require substantial upgrade of existing road infrastructure. In the future, we recommend analyzing higher level coordination strategies that help CACC vehicles form strings based on their routes. In addition, as the CACC market penetration increases, it is unlikely that the CACC is the only advanced traffic technology implemented. Systems such as the automated merging or lane changing assistance, and speed harmonization are likely to be deployed together with CACC. For this reason, we should also explore the impact of those systems on the CACC vehicle string operation.

REFERENCES

Dey, K. C., Yan, L., Wang, X., Wang, Y., Shen, H., Chowdhury, M., ... & Soundararaj, V. (2016). A review of communication, driver characteristics, and controls aspects of cooperative adaptive cruise control (CACC). *IEEE Transactions on Intelligent Transportation Systems*, *17*(2), 491-509.

HCM 2010: Highway Capacity Manual. 2010. Transportation Research Board of the National Academies, Washington, D. C.

Larson, J., Krammer, C., Liang, K., and Johansson, K. (2013). Coordinated Route Optimization for Heavy-duty Vehicle Platoons. *Proceedings of the 16th International IEEE Conference on Intelligent Transport Systems.* Hague, Netherlands, October 6-9.

Larson, J., Liang, K.-Y., Johansson, K.H. (2014). A Distributed Framework for Coordinated Heavy-duty Vehicle Platooning. Manuscript Accepted for Publication in *IEEE Transactions on Intelligent Transportation Systems.*

Liang, K.Y., Mårtensson, J., and Johansson, K. (2013). When is it Fuel Efficient for a Heavy Duty Vehicle to Catch Up With a Platoon? *Proceedings of the 7th IFAC Symposium on Advances in Automotive Control.* Tokyo, Japan, September 4-7.

Milanés, V., Shladover, S.E., 2014. Modeling cooperative and autonomous adaptive cruise control dynamic responses using experimental data. Transportation Research Part C: Emerging Technologies 48, 285-300.

Nowakowski, C., O'Connell, J., Shladover, S., and Cody, D. (2010). Cooperative Adaptive Cruise Control: Driver Acceptance of Following Gap Settings Less Than One Second. *Proceedings of the Human Factors and Ergonomics Society 54th Annual Meeting.* Santa Monica, CA: The Human Factors and Ergonomics Society.

Nowakowski, C., Shladover, S.E., Cody, D., Bu, F., O'Connell, J., Spring, J., Dickey, S., and Nelson, D. (2010). *Cooperative Adaptive Cruise Control: Testing Drivers' Choices of Following distances* (Technical Report for FHWA Exploratory Advanced Research Program Cooperative Agreement DTFH61-07-H-00038). Berkeley, CA: California PATH, Institute of Transportation Studies, University of California, Berkeley.

Shladover, S.E., Su, D., Lu, X., 2012. Impact of cooperative adaptive cruise control on freeway traffic flow. Transportation Research Record 2324, 63–70.

Su, D., Shladover, S., Lu, X.Y., and Nowakowski, C. (2011). *Impacts of Cooperative Adaptive Cruise Control on Freeway Traffic Flow* (Technical Report Contract Number: DTFH61-07-H-00038). Berkeley, CA: California PATH, Institute of Transportation Studies, University of California, Berkeley.

van Arem, B., van Driel, C.J.G., Visser, R., 2006. Impact of cooperative adaptive cruise control on traffic-flow characteristics. IEEE Transactions on Intelligent Transportation Systems 7 (4), 429–436.

VanderWerf, J., Shladover, S., Kourjanskaia, N., Miller, M., and Krishnan, H. (2001). Modeling Effects of Driver Control Assistance Systems on Traffic. *Transportation Research Record No. 1748.* Washington DC: Transportation Research Board, pp. 167 – 174.

VanderWerf, J., Shladover S., Miller, M., and Kourjanskaia, N. (2002). Effects of Adaptive Cruise Control Systems on Highway Traffic Flow Capacity. *Transportation Research Record No. 1800.* Washington DC: Transportation Research Board, pp. 78-84.

Yeo, H., et al. Oversaturated Freeway Flow Algorithm for Use in Next Generation Simulation. *Transportation Research Record: Journal of the Transportation Research Board* #2088, TRB, Washington, D.C., 2008, pp. 68-79.